UNIVERSITÀ DI PISA

Dottorato in Fisiopatologia Clinica

Ciclo XXXII

"Elucidating the role of Extracellular Vesicles on Pulmonary Arterial Smooth Muscle Cells - Pulmonary Arterial Endothelial Cells crosstalk in Human Pulmonary Arterial Hypertension using novel cutting-edge technologies to image functional cargo transfer"

PhD Candidate

Ilaria Passalacqua

Supervisor

Prof. Alessandro Celi

Anno accademico 2018 / 2019

Abstract

Pulmonary arterial hypertension (PAH) is a pathology characterized by acute remodelling of distal pulmonary arteries, right ventricular dysfunction, and increased pulmonary vascular resistance that promotes heart failure. Additionally, heritable PAH is caused by a mutation that results in impairment of the TGFβ superfamily signalling pathway. Previously considered as a largely untreatable disease, recent studies have utilised TGFβ1 treatment of Human Pulmonary Arterial Smooth Muscle Cells (HPASMCs) to mimic *in vitro* the mechanisms underlying PAH disease. Although extracellular vesicles (EVs) have been shown to influence the vascular environment, their role remains obscure for many pathologies. Recent work in Prof. Baker's laboratory demonstrated that EVs are involved in communication within vascular cells during PAH.

The aim of this project has therefore been to try and assess whether EVs from HPASMCs treated with an excess of TGFβ1 are involved in transporting functional cargo to Human Arterial Endothelial Cells (HPAECs) and whether this cargo may affect the latter within the vascular microenvironment of PAH.

In order to demonstrate the transfer of mRNA and its translation into protein during EVs uptake, a Cre-Lox*P* method optimised for its use in primary cell cultures was assessed. With this method, we were able to determine whether HPAECs had taken up EVs released by HPASMCs during PAH-simulated cell co-cultures. The method is as simple theoretically as difficult to reproduce practically. The method´s design is to enclose Cre mRNA upon donor HPASMC EVs while recipient cells (HPAECs) show whether Cre^{+} EVs have been taken up by switching from red to green fluorescence. Fluorescence-activated cell sorting of eGFP out of DsRed positive cells (ratio of 1.53±0.26%) demonstrated that using our Cre-Lox*P* system we could observe the transfer and translation of Cre-mRNA into protein from HPASMC-EVs to HPAECs. Interestingly, this transfer was re-

lated to TGFβ1 treatment which resulted in the marked increase of EVSuptake from HPAEC but not an increase in the number of EVs released by HPASMCs.

Single-stranded low-input RNA-Seq was used to characterise HPASMC-EVs´ cargoes. The cargoes present in EVs from Control and TGFβ1 treated HPASMCs were also been analysed, measuring 2417 differentially expressed transcripts in HPASMC-EVs. Among these, a subset of 759 RNAs was found significantly enriched, in Control EVs when compared to their donor cells. Particularly interesting was the finding of overexpressed GDF11, TGFβ3 and Zeb1 transcripts, that was further investigated. Furthermore, EVs from TGFβ1 treated cells showed 90 differential transcripts when compared to Control EVs. Gene Ontology Enrichment Analysis showed that these transcripts were typically associated with cellular differentiation, migration, and response to wounding: all mechanisms associated with PAH development and/or PAH-related EndMT. Some of these genes involved in EndMT have been validated also by means of qRT-PCR, such as palladin and bHLHE40 that were found over-represented in HPASMC-EVs.

Preliminary experiments showed that, after treating HPAECs with HPASMC-EVs, their cellular phenotype changed clearly at visual examination under the microscope; although, this behaviour needs to be investigated further. In summary, the present results illustrate the potential role for EVs during PAH pathogenesis. The *in vitro* Cre-Lox*P* system optimised for primary cells showed that HPASMC-EVs can release functional cargo. The transcriptomic data showed differential regulation of several transcripts that are critical for the remodelling of the vasculature during PAH development, as pilot experiments on HPAECs treated with HPASMC-EVs pointed out. However, more research on these preliminary results needs to be undertaken to better define the association between HPASMC-EVs uptake and PAH.

Table of Contents

Table of Contents

Table of Contents

Figures and Tables Index

Figures and Tables Index

1 Introduction

1.1 Pulmonary Arterial Hypertension

Pulmonary hypertension (PH) is a progressive occlusive vasculopathy in the lung, associated with abnormal vasoconstriction, excessive vascular wall remodelling, inflammation and *in situ* thrombosis. Increased vascular resistance accounts for a sustained elevation of blood pressure in the pulmonary circulation, leading to increased afterload for the right ventricle and eventually to right heart failure. The clinical manifestations of pulmonary hypertension are non-specific. The patients may have cardiopulmonary symptoms, e.g. dyspnea, chest discomfort, decreased appetite, fatigue, dizziness, and irregular heartbeat. The diagnosis of pulmonary hypertension requires a thorough physical examination and extensive tests including Doppler echocardiography and pulmonary function tests. The diagnosis should in most cases be confirmed by right heart catheterization, which when positive shows a mean pulmonary arterial pressure ≥ 25 mmHg at rest.

Pulmonary hypertension (PH) has been classified by the *World Health Organization (WHO)* based on the differing pathophysiologic mechanisms [1]. Group 1 categorizes PH that results from an abnormality of the arterial circulation, predominantly at the level of the precapillary bed, and thus is named *Pulmonary Arterial Hypertension*.

Other groups include: Pulmonary Venous Hypertension, which contains one of the most common forms of PH, congestive heart failure; PH associated with respiratory diseases and hypoxemia; PH due to chronic thrombotic and/or embolic disease; and PH due to multi-factorial disorders such as Lymphangiomatosis.

1.1.1 Clinical classification of PH

The first classification of PH was proposed in 1973 at an international conference on primary PH (PPH) endorsed by the World Health Organization. In 1998, a clinical classification of pulmonary hypertension (PH) was developed (here below), categorizing PH into groups which share similar pathological and hemodynamic characteristics and therapeutic approaches. Last update was in 2018, during the 6th World Symposium held in Nice, France.

In addition, a functional classification of PAH, similar to the one from NYAH for the heart diseases, was developed to allow comparison of patients with respect to the clinical severity of their symptoms (Table 1).

Currently, PH is classified into 5 clinical groups according to pathology, pathobiology, genetics, epidemiology, and risk factors. A schematic classification of PH is described here below: particularly, this study will focus on *Group 1: Pulmonary Arterial Hypertension.*

Group 1: Pulmonary arterial hypertension (PAH)

1.1. Idiopathic (IPAH)

1.2. Heritable (HPAH)

1.2.1. BMPR2 mutation

1.2.2. Other mutations

1.3. Drugs or toxins induced

1.4. Associated with:

1.4.1. Connective tissue disease

1.4.2. Human immunodeficiency virus (HIV) infection

1.4.3. Portal hypertension

1.4.4. Congenital heart disease

1.4.5. Schistosomiasis

2. Group 2: Pulmonary hypertension due to left heart disease

2.1. Left ventricular systolic dysfunction

2.2. Left ventricular diastolic dysfunction

2.3. Valvular disease

2.4. Congenital/acquired left heart inflow/outflow tract obstruction and congenital cardiomyopathies

2.5. Congenital/acquired pulmonary veins stenosis

3. Group 3: Pulmonary hypertension due to lung disease and/or hypoxia

3.1. Chronic obstructive pulmonary disease (COPD)

3.2. Interstitial lung disease

3.3. Other pulmonary disease mixed restrictive and obstructive pattern

3.4. Sleep-disordered breathing

3.5. Alveolar hypoventilation disorders

3.6. Chronic exposure to high altitude

3.7. Developmental lung diseases

4. **Group 4: Chronic thromboembolic pulmonary hypertension and other pulmonary artery obstructions**

    4.1. Chronic thromboembolic pulmonary hypertension (CTEPH)

    4.2. Other pulmonary artery obstructions

        4.2.1. Angiosarcoma

        4.2.2. Other intravascular tumours

        4.2.3. Arteritis

        4.2.4. Congenital pulmonary arteries stenoses

        4.2.5. Parasites (hydatidurias)

5. **Group 5: Pulmonary hypertension with unclear and/or multifactorial mechanisms**

    5.1. Haematological disorders: haemolytic anaemia, myeloproliferative disorders, splenectomy

    5.2. Systemic disorders: sarcoidosis, pulmonary histiocytosis, lymphangioleiomyomatosis neurofibromatosis

    5.3. Metabolic disorders: glycogen storage disease, Gaucher disease, thyroid disorders

    5.4. Others: pulmonary tumoral thrombotic microangiopathy, fibrosing mediastinitis, chronic renal failure (with/without dialysis), segmental pulmonary hypertension.

Table 1 - Functional classification proposed for PAH

Class I	Patients with pulmonary hypertension without resulting limitation of physical activity. Ordinary physical activity does not cause undue dyspnoea or fatigue, chest pain or near syncope.
Class II	Patients with pulmonary hypertension resulting in slight limitation of physical activity but comfortable at rest. Ordinary physical activity causes undue dyspnoea or fatigue, chest pain or near syncope.
Class III	Patients with pulmonary hypertension resulting in marked limitation of physical activity but comfortable at rest. Less than ordinary activity causes undue dyspnoea or fatigue, chest pain or near syncope.
Class IV	Patients with pulmonary hypertension with inability to carry out any physical activity without symptoms. Patients manifest signs of right heart failure. Dyspnoea and/or fatigue may even be present at rest. Discomfort is increased by any physical activity.

1.1.1.1 Group I: Pulmonary Arterial Hypertension

This group is represented by Pulmonary Arterial Hypertension (PAH) forms, also known in the past as Primary Pulmonary Arterial Hypertension (PPAH). Depending on its origin can be classified as: A) Heritable PAH: due to genetic mutations; B) Idiopathic PAH (IPAH): induced by drugs or toxins, which develops from unknown causes, and C) Associated PAH (APAH): develops secondary to an existing ailment such as a connective tissue disease, congenital systemic-to-pulmonary shunts, portal hypertension and HIV infection [4].

1.1.1.1.1 Idiopathic PAH

Idiopathic PAH causes are still unknown although it affects predominantly women (female-male ratio, 3:1). There are several reasons for patients to develop PAH, but in the absence of any demonstrable risk factors, they are labelled as idiopathic PAH (IPAH) [1]. It first presents with dyspnoea on modest exertion, loss of energy, and signs of right ventricular strain. There are familiar or sporadic forms: the first one occurs in almost 6% of IPAH cases and the incidence is likely higher, and it is also called *Familial or Heritable PAH*. Treatment with newer vasodilators and antiproliferative agents, such as prostacyclin salts, has improved functional capacity and prolonged mean survival from 3 to 6 years. [3]

1.1.1.1.2 Heritable PAH (HPAH)

Heritable PAH was recognized in the mid-1980s, and in 2000 (Figure 1) was linked to mutations in the *Bone morphogenetic protein receptor type II (Bmpr2) gene* and, more rarely, in the *Activin receptor-like kinase 1 (Alk1) gene* [2]. However, only 20% of those genetically at risk, with Bmpr2 mutations, develop PAH [3]. Recently (2013) a new mu-

tation on KCNK3 and TBX4 genes involved in the development of PAH, has been discovered.

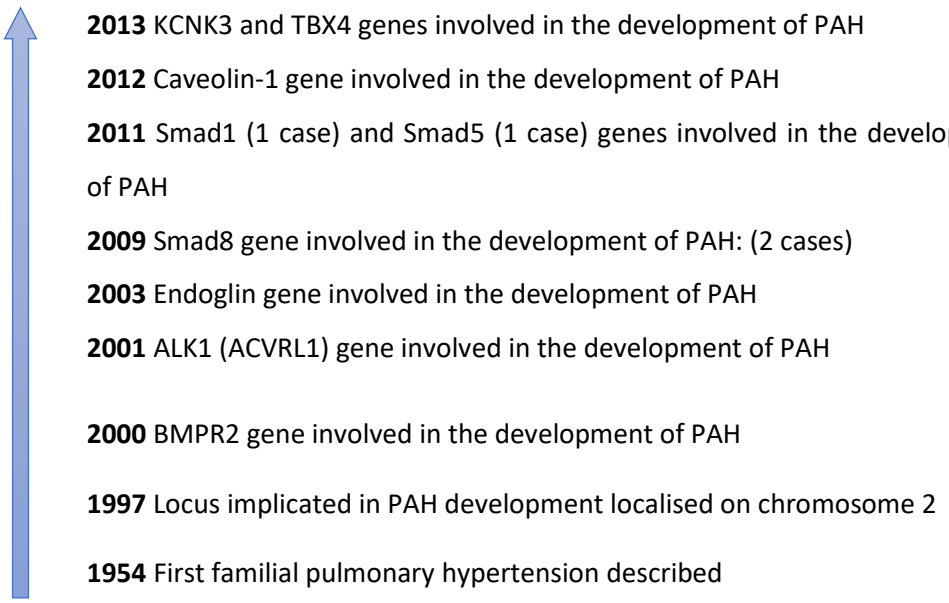

Figure 1 - Chronological discovery of gene mutations related to development of PAH

1.1.1.1.2.1 The genetics of PAH

Heritable PAH is an autosomal dominant disease with incomplete penetrance and an estimated lifetime risk of 10% to 20% [2]. The genetics of PAH is constantly evolving with a host of germline mutations being reported to date. Initial work in the 1990s and early 2000s highlighted that altered BMPRII signalling is a major risk factor for the development of PAH via BMPRII gene mutations [4][5][6] and it is more frequent in women than men, (1,7:1 ratio) [7][8]. Almost 20% of cases previously thought being IPAH have been investigated, further finding mutations in BMPR2 gene and therefore pose a hereditary risk to other family members. However, BMPR2 mutations have not been

identified in PAH associated with HIV or sclerosis. Here below, are the most important genes involved in the PAH pathogenesis:

1.1.1.1.2.2 TGFβ superfamily

TGFβ is the founding member of the TGFβ superfamily comprised of over 30 peptide cytokines in mammals including activins, inhibins, BMPs, and TGFβs. Members of the TGFβ superfamily are characterised by a cysteine 'knot' of six of these residues at the carboxyl-terminal [9].

Members of the TGFβ family are widely expressed in diverse tissues and play an essential role throughout life, starting from gastrulation and the onset of body axis asymmetry to organ-specific morphogenesis and adult tissue homeostasis [10]. TGFβs are synthesised, from the beginning of gastrulation processes in embryos, by many cell types (e.g. macrophages and fibroblasts) as inactive precursor proteins, which are modified intracellularly and then secreted as a latent complex [11][12]. At the cellular level, TGFβ superfamily members regulate fundamental cell processes such as proliferation, differentiation, death, cytoskeletal organization, adhesion, and migration [9].

1.1.1.1.2.2.1 Molecular pathway of TGFβ family members

The signalling of all the TGFβ superfamily members starts on the membrane by coupling to a receptor, ends at the nucleus with the recruitment of specific transcription factors and is transmitted by activating a series of serine-threonine (Ser-Thr) kinases (Figure 2 – Modified from Rol et al., 2018 - TGFβ superfamily signalling in PAH. In the case of the TGFβ ligands, the molecule binds to the serine/threonine kinase receptor TβRII and, in turn, TβRI (ALK5) is recruited, forming a heterotetrameric complex. In HPASMCs, this leads to the activation of the canonical Smad signalling pathway via Smads 2 and 3. Dif-

ferently, BMP ligands bind the BMPRII receptor and, in turn, recruit either ALK3 or ALK6, leading to the activation of Smads 1, 5 and 8. In addition to the activation of the canonical Smad signalling pathway by members of the TGFβ superfamily, non-canonical signalling pathways include members of the mitogen-activated protein kinases (MAPKs), such as p38 MAPK, p42/44MAPK (ERK1/2), and c-JunN-terminal kinase (JNK) areactivated by members of this family [10]. An important role in vascular remodelling has been given to the TGFβ superfamily signalling, in fact, it is considered a master regulator of EndMT [28].

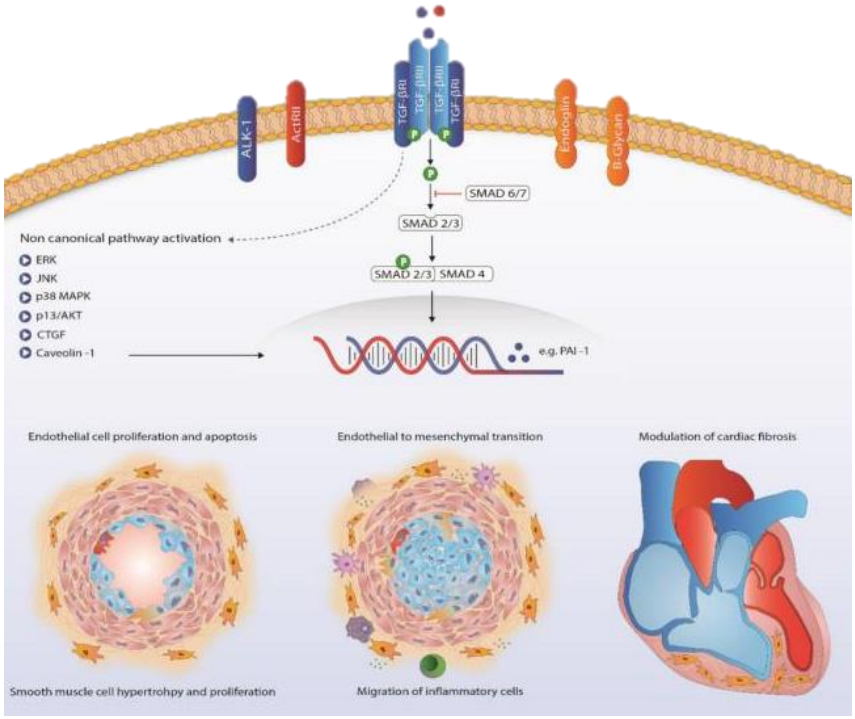

Figure 2 – Modified from Rol et al., 2018 - TGFβ superfamily signalling in PAH

1.1.1.1.2.2.2 Impairment of TGFβR and BMPRII in PAH

TGFβ is a pleiotropic cytokine involved a multitude of biological processes. Deregulation of TGFβ signalling has been observed in several diseases, such as fibrosis and cancer [13] and it has been also demonstrated to be involved in the development of PAH [10]. The exact rate of BMPRII mutations in the general population is not known but it is believed to be quite low. In HPAH, around 70% of patients display BMPRII mutations. BMPRII mutations are also reported in IPAH and around 15% of IPAH patients have these mutations [9]. These studies highlighted the importance of the TGFβ superfamily signalling and focused future studies to investigate this pathway in more detail. These genetic studies highlighted that ALK-1, endoglin and Smad9 mutations are also linked to the development of PAH and all of these mutations are members of the TGFβ superfamily. To summarise, the imbalance of the TGFβ1 – BMPRII signalling is the main cause for the altered phenotype associated with pulmonary arterial hypertension [5][6].

1.1.1.1.2.3 KCNK3 and Caveolin genes

The development of screening technologies has also led to the discovery of other mutations associated with PAH, for example, the KCNK3 gene (Potassium channel, subfamily K, member 3) and the caveolin-1 gene (CAV-1) [4]. The number of CAV-1 mutants with PAH is low but there is still an association and increased risk of developing PAH. Interestingly a reduction of caveolin-1 expression has been previously reported in the lungs of PAH patients and caveolin-1 has been reported to alter TGFβ signalling and reduce BMPRII signalling [16]. This mutation again highlights the importance of the TGFβ superfamily in the development of PAH.

1.1.1.1.3 Drugs or toxins induced PAH

A number of drugs and toxins have been identified as risk factors for the development of PAH and were included in the classification shown in Table 2.

Risk factors may include drugs and chemicals, diseases, or phenotype (age, gender). Risk factors are categorized as: definite, very likely, possible, or unlikely, based on the strength of their association with PH and their probable causal role (Table 2 - Risk Factors for and Associated Conditions of PAH).

Table 2 - Risk Factors for and Associated Conditions of PAH

Updated Risk Factors for and Associated Conditions of PAH			
Definite	**Possible**	**Likely**	**Unlikely**
Aminorex	Cocaine	Amphetamines	Oral contra-ceptives
Fenfluramine	Phenylpropanolamine	L-tryptophan	Estrogens
Dexfenfluramine	St. John's Wort	Methamphetamines	Cigarette smoking
Toxic rapeseed oil	Chemotherapeutic agents	/	/
/	Selective serotonin reuptake inhibitor	/	/

1.2 Vascular remodelling during PAH

Pulmonary hypertension (PH) refers to hemodynamic alterations of the pulmonary circulation in which the pulmonary arteries and veins undergo several structural alterations; those alterations have been recognized as pulmonary vascular remodelling and are frequently heterogeneous molecularly [1]. Alterations in cross-talk between HPAECs and HPASMCs are critical to pulmonary vessel re-

modelling.[17]. Pulmonary vascular remodelling likely contributes to increased pulmonary vascular pressures by increasing pulmonary vascular resistance. The remodelling process is typically accompanied by endothelial dysfunction, activation of fibroblasts and smooth muscle cells, crosstalk between cells within the vascular wall (EVs-dependent or independent), and recruitment of circulating progenitor cells.

Endothelial cells are known to be key regulators of vascular function. Indeed, during development, factors derived from endothelial cells are known to participate in blood vessel formation and maturation by recruiting and stabilizing vascular wall´s cells [18]. Diversely, during endothelial dysfunction, the production of either vasoconstrictors or vasodilators results imbalanced similarly to activators and inhibitors of smooth muscle cell proliferation and migration [14].

Cells isolated from normal subjects show BMPs signalling activation, inhibiting proliferation and inducing apoptosis in HPASMCs while enhancing survival in HPAECs and endothelial progenitor cells [19].

Contrarily, activated endothelial cells produce growth factors (VEGF, PDGF, FGF) promoting angiogenesis, vasoconstrictors and vasodilators (augmented production of *endothelin-1, ET-1* and *serotonin, 5-HT*) and cytokines, pushing the balance on the dysfunctional plate.

Because of HPAECs and HPASMCs closeness in the vessel bed, they can communicate one with another easily. Therefore, HPAECs secretion causes a proliferative and migratory arrangement of HPASMCs in the vessel wall by increasing intracellular $Ca2^{+}$; Also, HPAECs can realise vasoconstrictors inducing a “pseudo-hypoxic environment” and consequently the activation of *hypoxic induction factor – 1, HIF-1* a transcription factor composed by two subunits containing bHLH-PAS domains that bind DNA [20]. Multiple HIF-1 target genes play a key role in the re-

sponse of HPASCMs to hypoxia. Two of these genes are KCNA5 and KCNB1 codifying for *voltage-gated K^+ channels: an enhancement of K^+ channels expression* lead to an increase in proliferation and a decrease in apoptotic events in HPASMCs [21]. These mechanisms are simplified in Figure 3.

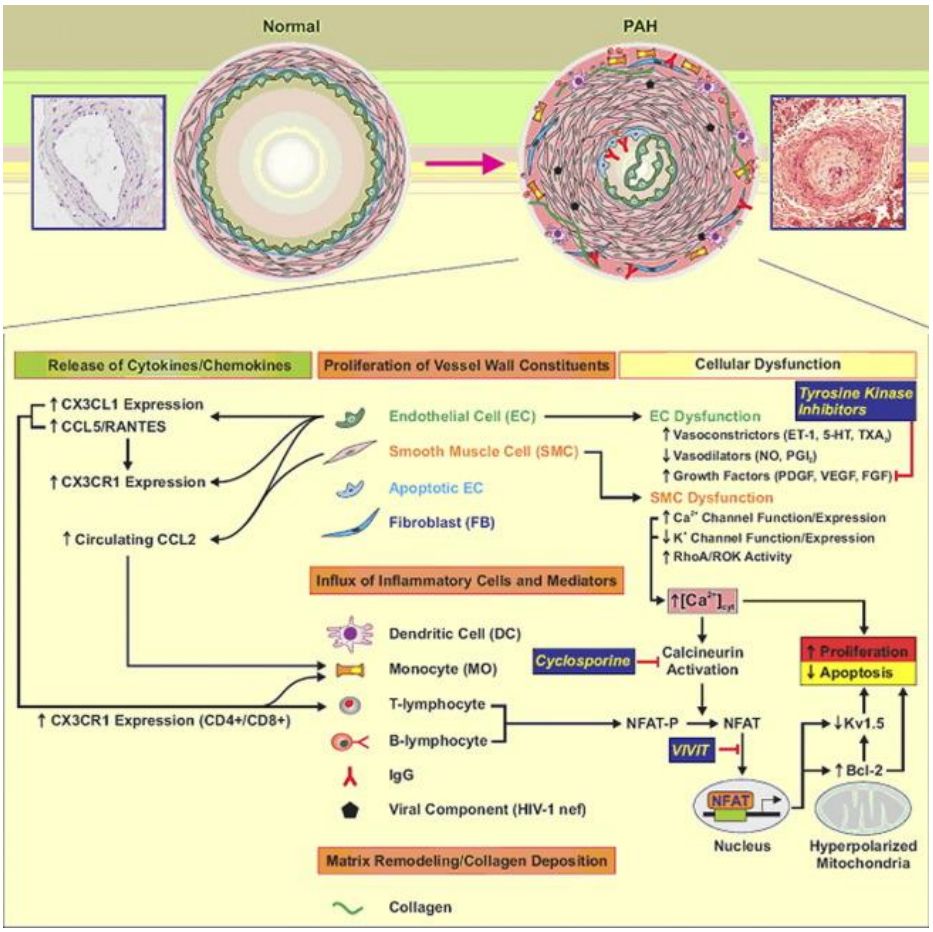

Figure 3 - Molecular mechanisms of inflammation-mediated remodelling during PAH (Modified from Hassoun PM et al.,) - These schematic features, (inflammatory mediators, cells, and mechanisms involved in pulmonary vascular remodelling) mediate the influx of inflammatory cells and cellular dysfunction, and contributes to release vasomotor and growth mediators as well as the activation of transcriptional factors.

1.2.1 Endothelial-to-Mesenchymal Transition in PAH

Endothelial-to-mesenchymal transition (EndMT) is a process whereby an endothelial cell undergoes a series of molecular events that lead to change their characteristic cobblestone morphology towards a mesenchymal phenotype (Figure 4). However, at a molecular level, there are still no agreed criteria for defining EndMT.[22] During this process, endothelial cells progressively lose their characteristics, (e.g., cell-cell junctions and specific markers such as CD31 and VE-cadherin), gain mesenchymal markers giving them a contractile phenotype, such as α-SMA, SM22 α and collagen-I, and ultimately migrate and invade the surrounding tissues [23] (as better shown in Figure 5).

TGFβ is the most well-known EndMT inducer and upregulates the expression of transcription factors, such as SNAIL, SLUG, and ZEB1. These transcription factors then upregulate the expression of mesenchymal markers. [23][22], However, cell signalling associated with inflammation-induced EndMT remains still poorly understood. Although EndMT is involved in many pathologies (e.g. cardiovascular and cancer), it also plays a fundamental role during cardiac development [24].

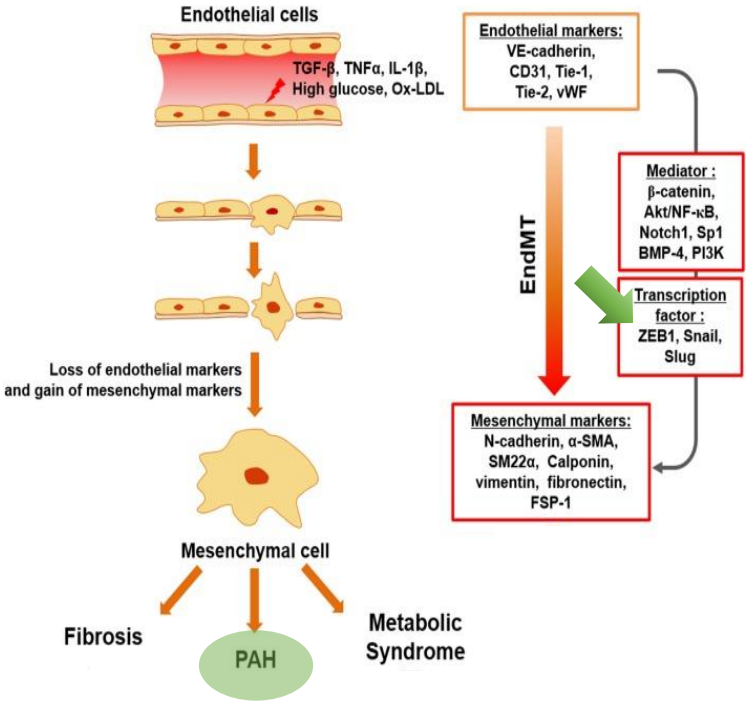

Figure 5 - EndMT and its inducing factors (Modified from Cho JG, et al. 2018)

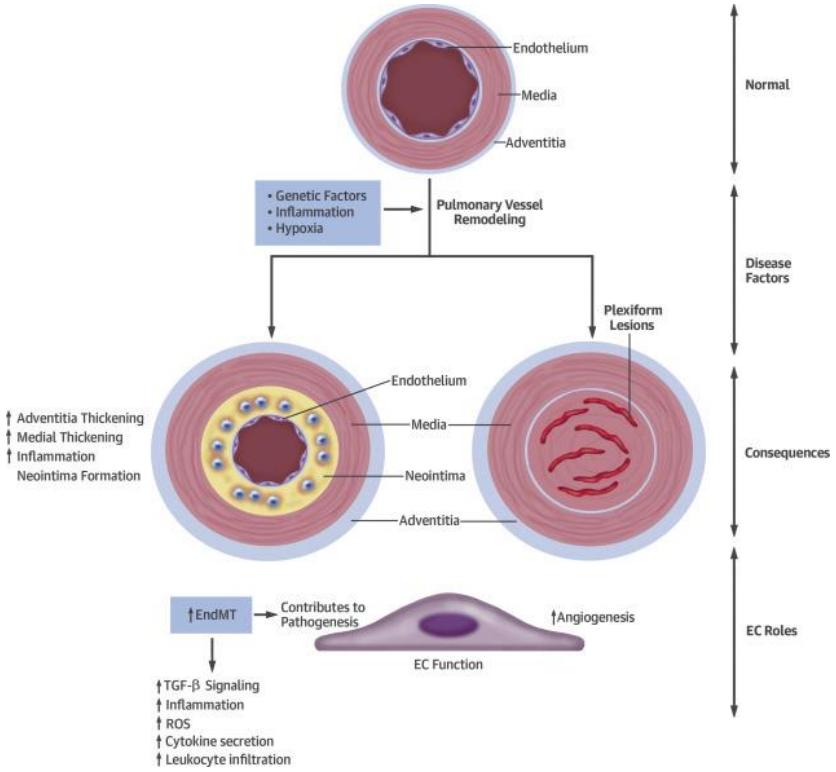

Figure 4 - Endothelial-to-Mesenchymal Transition in PAH (from Kovacic JC, et al.)

1.3 Extracellular Vesicles

Extracellular vesicles (EVs) consist of a small lipid bilayer surrounding and contain proteins, lipids, metabolites, and nucleic acids [25]. Virtually all eukaryotic cells shed submicron vesicles constitutively, upon activation or during apoptosis. EVs vary in size, composition and mechanisms of generation, and depending on these characteristics they are usually distinguished into *exosomes* (Exo), *microvesicles* (MVs, also called microparticles or ectosomes) and *apoptotic bodies* (Figure 6) [26]. They may be released and taken up by many cell types, including bacteria and plant cells, which makes cross-communications very likely [22].

While their existence has been known for a long time, these structures were initially considered laboratory artefacts or cell debris with no physiological significance. Nevertheless, researchers began to be interested in their potential role in physiology and pathophysiology, finding them to be involved in processes as diverse as, for instance, blood coagulation, inflammation, and tumour cell growth. EVs have also been recently demonstrated to be essential mediators of cell-to-cell communication [26].

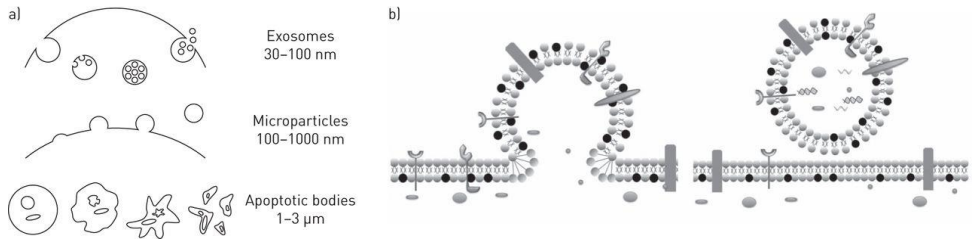

Figure 6 - Structures and categories of EVs (from Nieri D. et al. 2016)

1.3.1 Biomarkers for PAH

Ideally, a biomarker should be a surrogate for clinical endpoints that is observer-independent, widely available, non-invasive, disease-specific, a sign of disease activity, a target for treatment, and statistically significant.

In an effort to bypass these limitations, a number of circulating biomarkers have been investigated in PAH as potential objective and non-invasive tools for diagnosis, prognosis, and response to therapy and they could be summarised as follows:

- biomarkers of dysfunction (natriuretic peptides, endothelin ET-1);
- myocardial injury (troponins);
- inflammation/oxidative stress (interleukins IL, C-reactive protein, isoprostanes); vascular damage/remodelling (von Willebrand factor vWF, angiopoietin Ang, Extracellular Vesicles , Growth differentiation factor-15 GDF-15);
- end-organ failure (creatinine, sodium, uric acid); and transcriptional regulators;
- gene expression (miRNA, provirus integration site for Moloney murine leukaemia virus-1, PIM-1)[28].

Thus, there are a number of biomarkers which are strongly associated with PAH, although they might not be as useful in the diagnosis of PH, since they are not specific of the pathology but rather from some of its associated consequences: overproduction of ET-1 [29], increased incidence of pulmonary thrombosis, high levels of inflammatory cytokines such as interleukin-1 (IL-1) and IL-6 [30], [31] [32] as well as structural changes to the pulmonary vasculature [33][34]. Most of these biomarkers are associated with vasculature remodelling.

1.3.1.1 EVs as potential therapeutics and biomarkers for PAH

EVs can contain various macromolecules including proteins, lipids, and nucleic acids such as microRNAs. EVs can act as positive or negative modulators of cardiovascular diseases depending on the type and state of the cells from which they can originate. For example, EVs contribute to atherosclerosis progression and plaque rupture promoting microcalcification [35] and, in contrast, certain EVs have beneficial effects on vascular function and endothelial regeneration [36][37].

Currently, used biomarkers are not powerful in determining PAH onset, and hence other potential and more accurate biomarkers are needed. In fact, it has been studied whether ncRNAs, such as miRNA and lncRNA, could represent an advantageous strategy to identify promptly PAH through a simple blood test [38][22]. Most studied miRNAs involved in PAH onset and progression are: miR-143/145, miR-30, miR-21, miR-23a. These miRNAs are still under investigation, and it seems they might be transferred from cell to cell, being enclosed into EVs and released inside the appropriate recipient cells as in the case of mIR-143-3p, which has been seen to be transferred by HPASMC-EVs and play a crucial role in the progression of PAH [39] – see Figure 7.

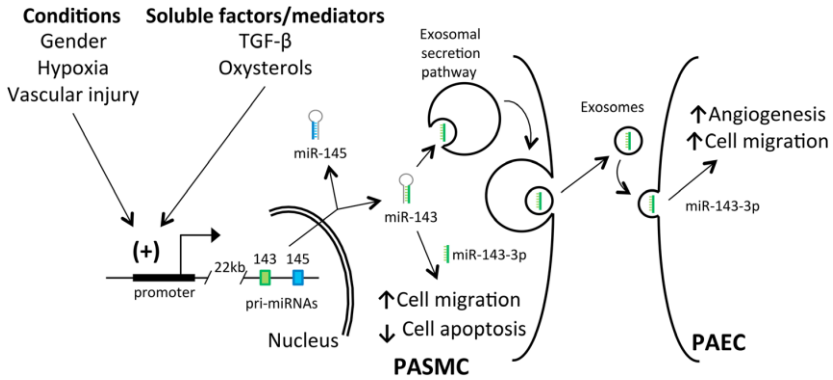

Figure 7 - Representation of miR-143-3p transported by HPASMCs-EVs and taken up by HPAECs (from Deng et al., 2015)

However, another interesting approach would be exploring the mechanisms involved behind the EVs´ release and their cargo, and how these could be connected to such pathology. Many publications have already reported the involvement of EVs in PAH [30][32] and also, how they can represent a therapeutic way to ameliorate some pathological status connected to PAH (such as endothelial dysfunction) [43][44].

1.3.2 The Cre-Lox*P* method to image the uptake of EVs: *in vitro* and *in vivo* methods

The Cre-Lox*P* method conceived by *Zomer et al,* in the recent 2015, allows the detection of cells that take up EVs released by donor cells. Although other methods to image uptake have already been studied, such as fluorescently labelled EVs, these do not discriminate between functional mRNA uptake and non-functional mRNA uptake as in the case of lysosomal degradation. Moreover, labelling methods (such as PKH67 dye) often show false-positives due to the serum proteins micro-aggregates (coming from FBS use for culturing) resulting labelled and looking like EVs under the microscope [45].

Contrarily, this method gives the chance to specifically image functional uptake of EVs, release of their cargo in the cytoplasm and translation of mRNA (in this case, the Cre mRNA) within the recipient Reporter^{+} cells. In order to work, this cargo has to be actively functional in order to produce a colour switch: from red to green when Reporter^{+} cells take up Cre^{+}-EVs.

The mechanism behind it (Figure 8), is based on the fact that the transgenic construct internalised by Reporter cells is composed by a floxed DsRed gene followed by a stop codon and ending with an eGFP gene. Whenever the Cre recombinase

mRNA (produced by the donor cells and enclosed in Cre^+-EVs) is internalized and translated, it activates the cleavage on the Lox*P* sites and DsRed gene and stop-codon are removed from the construct leading to eGFP expression. This will turn the $Reporter^+$ cells from red to green fluorescent, indicating that the uptake has happened.

The Cre-Lox*P* method can be used to study both *in vitro* and *in vivo* EVs transfer [46], although results acquired with the *in vivo* Cre-Lox*P* method may lead to discrepancies compared with results obtained *in vitro*, when using purified EVs, and this might need to be taken into account.

The general experimental design is resumed here following:

- Producing Cre^+ cell lines;
- Analysis of EVs cargo for the presence of Cre;
- Producing $Reporter^+$ cell lines;
- Studying *in vitro* EVs transfer;

Recent studies used this novel methodology in disparate fields and applications, such as for visualising cancer-derived EVs transfer to other cancer cells [46] or from tumour to host cells and from brain cells to immune cells in mice, studying the effects of this transfer [47]. Despite the method being a powerful technique to study virtually any kind of communication EVs-mediated, it has only been used to date in cell lines or for *in vivo* experiments, but never before in primary cells *in vitro*.

The optimisation of this methodology, in order to be used in primary cells cultures, has been made at Prof. Baker's Laboratory by Dr Fernando De la Cuesta, with whom I had the pleasure to work with during my visit to the lab.

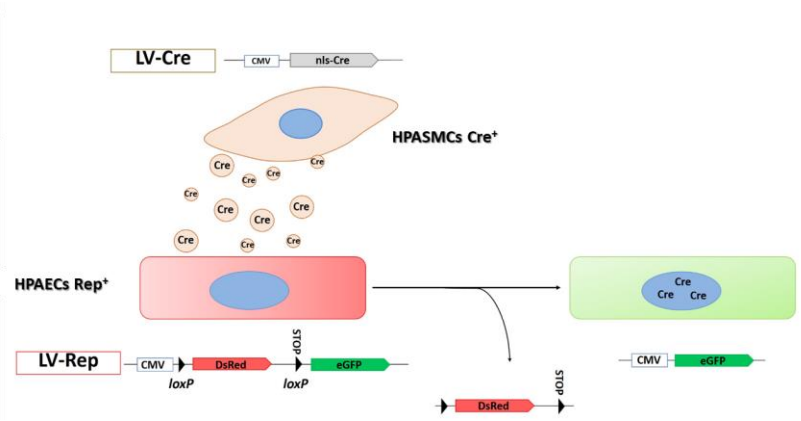

Figure 8 - Cre-LoxP method illustrated. Application on HPASMCs and HPAECs

2 Aim of the study

2.1 Hypothesis

Despite EVs having been studied for a long time now, their role in some pathologies appears obscure and it is still under investigation. Previous work from Prof. Baker's Lab [41] demonstrated the involvement of HPASMC-EVs loaded with miR-143 during PAH. TGFβ is considered one of the master regulators of EndMT and its signalling axis is impaired in heritable PAH. Therefore, it is here hypothesised that EVs may have a pathological role during PAH-associated EndMT by mediating cell-cell communication within the pathological microenvironment.

2.1.1 Objective

The main objective of this study is to elucidate and investigate the involvement of EVs during PAH, *in vitro* by:

1. ***Imaging the uptake*****:** Imaging HPAECs´ uptake of HPASMC-EVs using a primary cell Cre-Lox*P* method; Looking for phenotypic changes in HPAECs treated with HPASMC-EVs.

2. ***Analysing the cargo*****:** Assessing whether EVs derived from TGFβ1 treated HPASMCs are involved in transporting functional cargo to HPAECs; Validating enrichment or differential regulation of functional RNAs enclosed in HPASMC-EVs.

3 Materials and Methods

3.1.1 Cell cultures

Human pulmonary artery smooth muscle cells (HPASMCs) and pulmonary arterial endothelial cells (HPAECs) were purchased from Lonza and grown in Clonetics SmGM-s BulletKit medium (PromoCell) + 10% FBS, 1% L-Glut, 1% Pen-Strep, and EBM-2 Endothelial Growth Basal Medium (Lonza or PromoCell) + 10% FBS, 1% Pen-Strep, respectively.

In order to stimulate HPASMCs with TGFβ1, they were previously starved for 48h in MEM + 0.2% FBS and then incubated with TGFβ1 for 48h renewing stimuli the day after.

Meanwhile, HPAECs were starved for 24h in starvation media composed by EBM-2 with hydrocortisone and ascorbic acid from the kit + 1% FBS. After that HPAECs were treated or not with HPASMC-EVs suspended in MEM. The exo-free FBS, used to perform stimulation experiments, was depleted of EVs by overnight ultracentrifugation at 100,000 xg. For the EndMT model was conducted a 7 days-protocol with a combination of cytokines known to induce EndMT in complete EBM-2 + 20% exo-free FBS after 1-day starvation (as described in this chapter).

3.1.2 Co-cultures and Transwell co-cultures

For long-distance communication experiments, $9x10^4$ HPASMCs grown in full media were plated on the bottom of a 6 well plate and left grow for few hours / until the attached on the bottom in their own media, whether $3x10^4$ pulmonary arterial endothelial cells were plated on the inner face of a transwell 1 µM 6 well plates membrane from Corning, as shown in Figure 9.

Co-cultures were carried out in complete EBM-2 + 20% exo-free FBS.

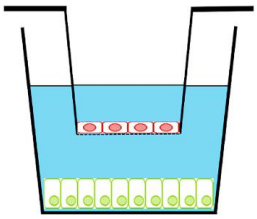

Figure 9 - Transwell co-cultures: distant co-culture

3.1.3 Cell cultures for EVs production

In order to produce a bulk amount of EVs, cells were seeded in several T175. When cells reached 70-80% confluence, either HPASMCs media (0.2% exo-free FBS) in combination with TGFβ1, was administered to allow the release of EVs from cells'membrane. The EVs would be released inside the medium and then recovered as follow.

3.1.4 Isolation of EVs and characterization methods

Isolation of EVs was made by cultivating HPASMCs (for HPASMC-EVs experiments) and collecting their culturing media (supernatant) to isolate EVs released into it. These supernatants were first centrifuged at 2000·xg for 10 mins at 4°C in order to remove dead cells and debris. Then, EVs were obtained after two consecutive steps of ultracentrifugation at 100,000·xg for 1h at 4°C in a Sorvall WX+ Ultracentrifuge using a TH-641 Swinging Bucket rotor (Thermo Fischer Scientific). Then were characterised using the following methods:

3.1.4.1 Nanoparticle tracking analysis (NTA)

NTA is a well-known and established method to estimate nanoparticles concentration, therefore it has been also applied for EVs works.

EVs were pelleted by ultracentrifugation was diluted 1:10 with PBS in order to be measured by NanoSight LM14 (Malvern Panalytical). An amount of 3-5 videos of 60 sec were acquired per each sample and included if only exceeding 500 particle tracks. EVs concentration (EVs/ml) was calculated as average of these technical replicates and normalised when used on a certain number of cells. At this point, EVs/cell was calculated.

3.1.4.2 Western Blot

Western Blots were performed to better characterise EVs profile by using typical EVs surface markers such as CD63, CD81, and CD9 [48]. In this case, CD63 was used as reference marker and Histone 3 as control for ruling out cell contamination. Protein lysates were obtained treating cell pellets with adjusted volume of 1X RIPA buffer then sonicated three times for 10 sec. Subsequently, they were resolved in 4-12% Bis-Tris Plus Gels using a Bolt Mini Gel Tank electrophoresis unit and run at a constant voltage of 200V/gel for 1h. Proteins were then transferred onto a nitrocellulose membrane under constant voltage (10V for 1h). Ponceau S (Sigma-Aldrich) staining was performed on the transferred membranes to ensure the uniform transfer of samples. Membranes were then blocked for 1h at RT using 5% dried non-fat milk (Blocking buffer). Mouse monoclonal (mouse mAb) anti-CD63 - ab59479 and rabbit polyclonal (pAb) anti-Histone 3 - ab70550, from Abcam were used as primary antibodies; also, mAb anti-GAPDH - D4C6R, and rabbit mAb anti-GAPDH - 14C10 from Cell Signaling Technology. Secondary anti-

bodies were purchased from LI-COR comprising: IRDye 800CW goat anti-mouse, IRDye 680RD goat anti-rabbit, IRDye 680RD goat anti-mouse and IRDye 800CW goat anti-rabbit.

After blocking the membranes, they were first incubated with the primary and then secondary antibodies, both for 1h in Blocking buffer. Detection was performed in an Odyssey imaging system (LI-COR).

3.1.5 Fluorescence-Activated Cell Sorting, FACS

Fluorescence-activated cell sorting (FACS) is a specialised type of flow cytometry that provides a method for sorting heterogeneous solutions of cells thanks to a specific light scattering capable to detect and divide the population of cells depending on their physical characteristics and fluorescent labelling. Indeed, fluorescent antibodies directed against surface molecules can be used to identify and quantitatively analyse specific cell phenotypes within a population of cells. Nowadays, FACS is one of the most e powerful methods utilised in science, for diagnostic, research or screening purposes. It is adaptable and it can be employed into disparate applications (i.e. characterise blood cells and for immunodiagnostics [49], identify tumoral cells [50], study the cell cycle [51], and many others). In this study, we used FACS to sort green from red fluorescent cells and create pure cell cultures avoiding background recombination events and estimate number of cells taking up EVs by the colour switch (e.g. Figure 17) during Cre-Lox*P* and quantifying GFP^+ cells in PKH67 experiments .

3.1.6 Total (miRNA enriched) RNA extractions

Total RNA enriched in miRNA used for validations was extracted using miRNeasy kit (Qiagen) as described here below.

Pelleted cells were previously treated with 700 µl QIAzol, homogenised and left at RT for 2 minutes. Then 140 µl of chloroform was added on top of each sample mixed for 15 seconds and then left 2 minutes at RT and centrifugated at 12000Xg at 4°C for 15 minutes. In the next step, the aqueous phase enriched in nucleic acids was collected (avoiding touching the white interphase and the pink phase containing organic solvents) and added to 1,5 volumes of ethanol into the column tube. About 700 µl of sample will be recovered from the previous step and used in two consecutive centrifugations: 8000Xg at R for 15 seconds, twice discarding the flow-through. DNase digestion was performed for cell samples but not for EVs samples in order to avoid losing material After this passage, 700 µl Buffer RWT was added to the column and span as before. Then two step of Buffer RPE centrifuge (500 µl) were completed. Finally, the column was let drying by spinning it for 1 minute and then the RNA was eluted in 20-40 µl of RNase -free water. The extracted RNA was quantified using Qubit technology (Thermo Fisher Scientific) and samples' quality was assessed using a Nanodrop 1000 (Thermo Fisher Scientific).

3.1.7 Gene expression quantitative Real Time-PCR (qRT-PCR)

For gene expression analysis, cDNA for mRNA analysis was obtained from total RNA using the Multiscribe Reverse Transcriptase (Life Technologies, Paisley, UK). qRT-PCR was performed using TaqMan primers or Power SYBR green (Life Technologies) with custom PCR primers (Eurofins MWG, Ebersberg, Germany). Ubiquitin C (UBC) or GAPDH were selected as housekeeping genes due to its stability across all groups studied, as checked on the RNA-Seq differential analyses. Primer and probes used in these experiments are shown in Table 3 and Table 4.

Table 3 - TaqMan Probes used to validate EVs' RNA cargo

Target	Gene Name	TaqMan Probe
bHLHE40	BHLHE40	Hs01041212_m1
Palladin	PALLD	Hs00363101_m1
Serpine1	SERPINE1	Hs01126606_m1
GDF11	GDF11	Hs00195156_m1
TGFβ3	TGFβ3	Hs01086000_m1
Zeb1	ZEB1	Hs01566408_m1

Table 4 - SYBr primers and TaqMan used to titre lentiviruses

Gene/Sequence	*Primer*	*TaqMan probe*	*SYBr Green*
LTR	**FW:**TGTGTGCCCGTCTG TTGTGT	**5'**-(FAM)-CAG-TGGCGCCCGAACAGGGA-**(TAMRA)-3'**	**RV:** GAGTCCTGCGTCGA-GAGAGC
Cre	**FW**:ATACCGGAGATCAT GCAAGC	/	**RV:**TTGCCCCTGTTTCACT ATCC

3.1.8 Immunocytochemistry (ICC)

In order to perform ICC, HPASMCs were pre-seeded on coverslips. After 24h, cells were fixed using 4% paraformaldehyde and permeabilized with 0.1 % Triton X-100 in PBS. To stain cytoplasmatic and nucleus components they were incubated 16 h at 4°C with the primary antibodies: mouse monoclonal to CD63 - ab59479, rabbit polyclonal to BMP11 (=GDF11), ab220951, rabbit polyclonal to TGFβ3, ab15537, from Abcam; and rabbit polyclonal to Zeb1, HPA027524 from Sigma-Aldrich while Phalloidin-iFluor 488 (Abcam) was used to counterstain the cell's cytoskeleton. After this step, coverslips were incubated with the secondary anti-bodies: goat anti-mouse Alexa Fluor 647 (Invitrogen), goat anti-rabbit Alexa Fluor

594 (Abcam). Nuclei were stained with DAPI. Cell preparations were visualized by means of TCS SP8 confocal microscope (Leica).

3.1.9 PKH67 labelling of EVs

PKH67 dye was used for EVs´ labelling. Dye was combined with EVs for 30 sec then quenched with 1% FBS and finally diluted with FBS-free MEM before being ultra-centrifugated at 100,000xg. The pellet was suspended in a small amount of FBS-free MEM and EVs/ml concentration was measured by NTA. An amount of $5x10^3$ HPASMC-EVs/cell was used to treat HPAECs for 20h. The negative control for the labelling procedure was obtained by performing the same procedure without EVs. Ultracentrifugation and addition to HPAECs of this negative control of PKH67 dye alone were carried out in parallel to check that the dye did not form aggregates or stained erroneously other proteins.

3.1.10 Lentiviral vectors production

Lentiviral vectors were produced by triple transient transfection of HEK293T cells using: a packaging plasmid (pCMVΔ8.74), a plasmid encoding the envelope of vesicular stomatitis virus (VSVg) (pMDG) (Plasmid Factory, Bielefeld, Germany) and a plasmid carrying the target gene, employing polyethyleneimine (PEI; Sigma-Aldrich, St Louis, USA) and the virus harvested by ultracentrifugation of the supernatant.

Lentiviral titres were determined by TaqMan quantitative real-time PCR (qRT-PCR) using probes lentivirus specific described in

Table 4. As plasmids carrying target gene, in this case, we used a Cre recombinase lentivirus (LV-Cre), produced using an LV-CMV-nlsCre plasmid (Plasmid #12265,

Addgene), while a reporter lentivirus (LV-Rep) was generated from the plasmid pLV.CMV.MCS.Lox*P*-DsRed-Lox*P*-eGFP, which was generously provided by Prof. Jacco Van Rheenen, Hubrecht Institute. (Both constructs are shown in Figure 10. An empty lentiviral vector (LV-CMV with no expression genes) was also produced to use as Null control for LV-Cre transduction.

3.1.11 Virus infections

Cells were plated 24h prior to infection, incubated with fresh media containing the appropriated multiplicity of infection (MOI)/ number of cells, incubated for 24h then washed and maintained until harvesting.

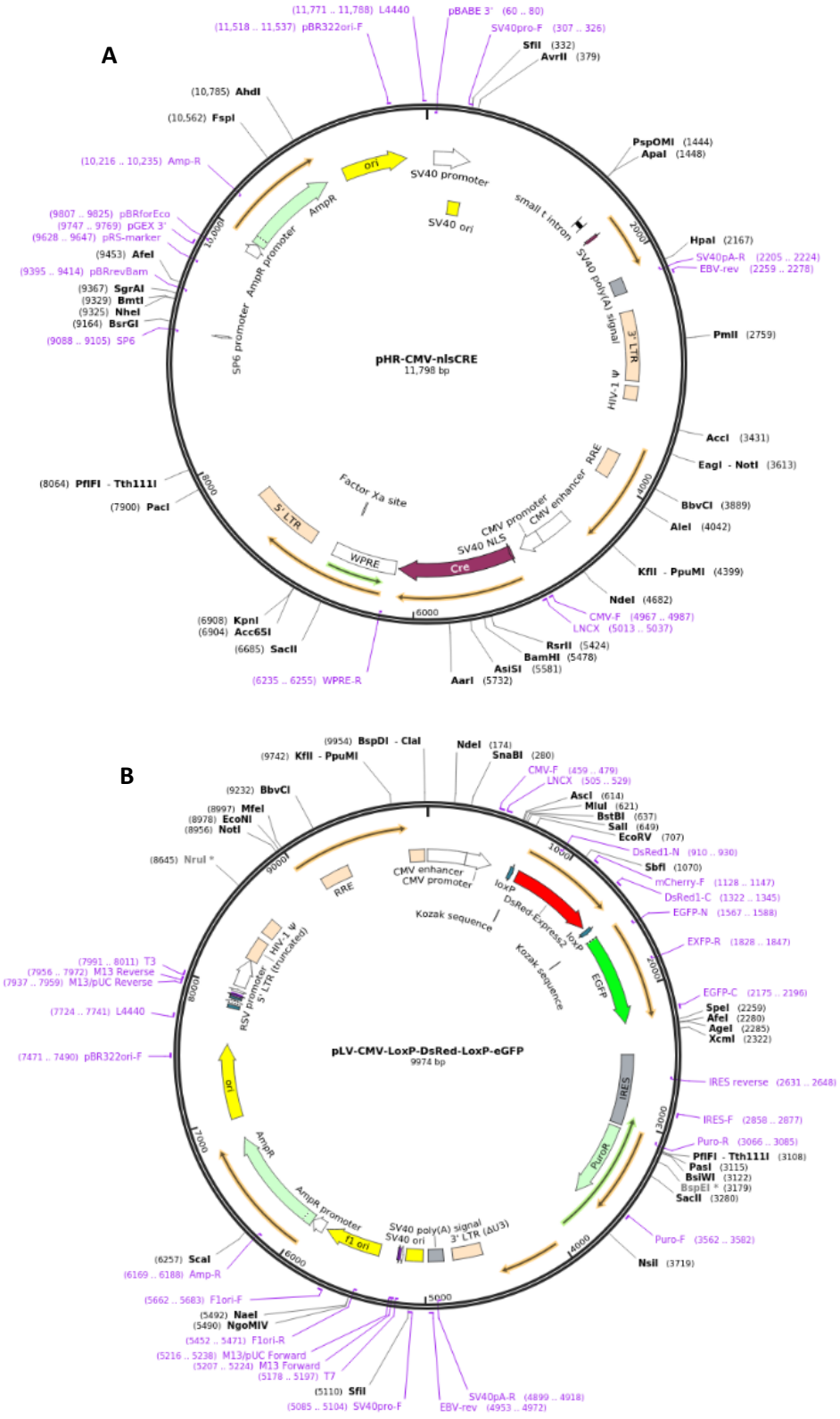

Figure 10 - Plasmid used for the Cre-LoxP method on primary cells: A. LV-Cre; B. LV-Rep

3.1.12 Modified Cre-Lox*P* method: application to primary cells

The previously described method [52] was used and modified in order to address the aim of visualising transfer of EVs into primary cells. This method had been used only on cell lines (mostly tumoral) and never on primary cells. Therefore, this protocol has been optimised by Dr Fernando De la Cuesta, in order to be shortened and used on primary cells (as their lifespan is shorter than that of cell lines) [53] Donor cells were transduced with Cre recombinase lentivirus created as described earlier. Then the presence of Cre mRNA into EVs released by those cells was confirmed by qRT-PCR. Recipient cells have been transduced with a Reporter lentivirus turning the recipient cells red fluorescent (LV-Rep).

The expression of Cre mRNA carried in HPASMC-EVs from HPASMCs transduced with LV-Cre (MOI 10) was confirmed by qRT-PCR, using SYBR green and the primers described on

Table 4 - SYBr primers and TaqMan used to titre lentiviruses and data are shown in Figure 11. After the virus infection with the above-described constructs, HPAECs Rep$^+$ were transduced by using an MOI 0.1 of LV-Rep in order to minimize background recombination. A series of MOI was first tried to select the one giving the best outcome (no background recombination).

Red fluorescent cells after 48-72h were sorted by means of FACS Aria Fusion sorter (BD Biosciences, San Jose, CA) and then incubated for 72h before starting co-cultures. During co-cultures, HPASMCs Cre$^+$ and HPAECs Rep$^+$ were cultured together in EBM-2 Endothelial Growth Basal Medium (Lonza or PromoCell) + 10% FBS, 1% Pen-Strep for 7 days. Recombination value was obtained by the %eGFP$^+$/DsRed$^+$ ratio, on a total amount of green/red fluorescence positive cells measured by FACS in LSR Fortessa (BD Biosciences) (Figure 11).

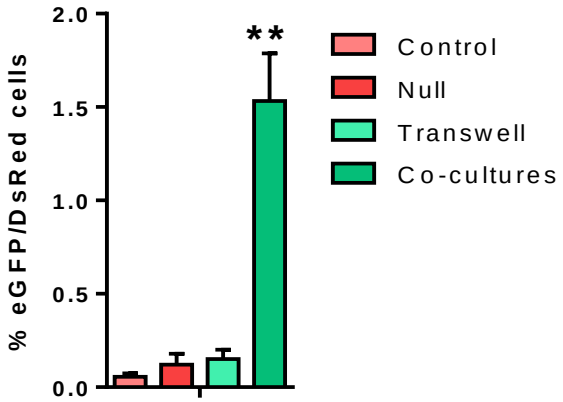

Figure 11- Transduction efficiency of HPAECs compared to the Control and Null.

A question that came spontaneously while carrying out the project was "Is the EVs transport uni- or bidirectional? Is it working sideways?". Hence, both HPAECs-HPASMCs and HPASMCs-HPAECs (with or without transwells membranes) communications were investigated. Therefore, it was also of interest to determine whether the efficiency was higher in one direction or another and to check the natural propensity of EVs to be taken up from a cell type or another.

3.1.13 Evaluation of the alteration of the uptake or translation levels from EVs-Cre in co-culture of cells.

The optimized primary cell Cre-Lox*P* system was also used to evaluate any alteration of uptake and translation of EV-mRNA by activated HPAECs *in vitro*. To pursue such investigation TGFβ1 (5 ng/ml) was tested as characteristic stimulus of PAH (*in vitro*). Stimulation was performed every 48h during the 7 days protocol. Quantification of Cre-induced recombination was assessed by FACS showing significant differences in TGFβ1 treated HPASMCs Cre^{+}: HPAECs Rep^{+} co-cultures as compared to the untreated.

3.1.14 Statistical analysis

Graphs' data were calculated as mean ± standard error mean (SEM). Comparisons between 2 groups were analysed using 2-tailed unpaired Student's t-test. All statistical analyses of qRT-PCR data were performed on the dCt scale and their graphical representation RQ±SEM was used. Validation of RNA-Seq data was performed by qRT-PCR and analysed by 1-tailed unpaired Student's t-test. Using Levene's test data were test prior to statistical analysis, finding none unequal variance between groups for any analyses of the dCt scale data. Statistical significance is indicated by a p-value of less than 0.05 and represented as follow: *P≤0.05, **P≤0.01, ***P≤0.001.

4 Results

4.1 Characterisation of HPASMCs derived EVs

To verify whether HPASMCs derived EVs were efficiently isolated, western blot was performed using CD63 as EVs marker and His3 as negative control (Figure 12A). GAPDH was used as positive control for cells´ lysate. Additionally, NTA analysis was performed confirming also the presence of EVs, which ranged between 80-500 nm as can be seen in Figure 12B. The average number of EVs was measured 3 times per sample and a number of $1x10^4$ EVs/cell was observed. Effectivness of TGFβ1 treatments performed on HPASMCs were verified by means of qRT-PCR on Serpine1, typical TGFβ1-downstream activated gene (not showed). ICC experiments have been performed as described in *Materials and Methods* chapter to also show localization of EVs inside HPASMCs, before being released (Figure 13).

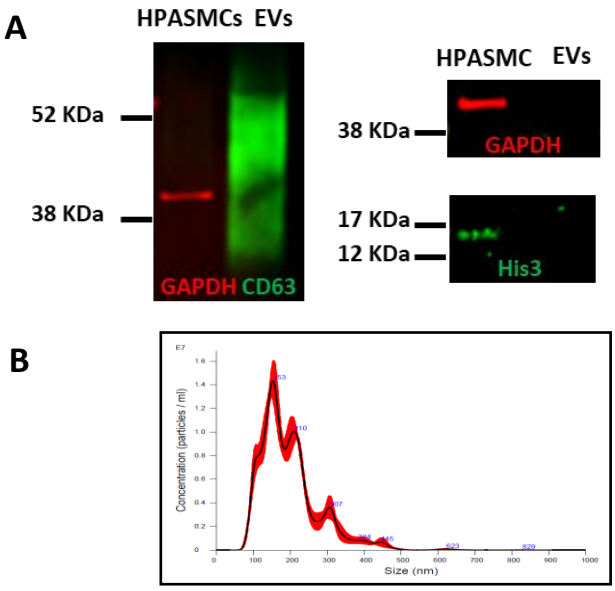

*Figure 12 - Characterisation of EVs; **A**, WB shows the typical EVs' smear; **B**, The bar graph represent concentration of EVs per cell in Control and TGFβ1 samples;*

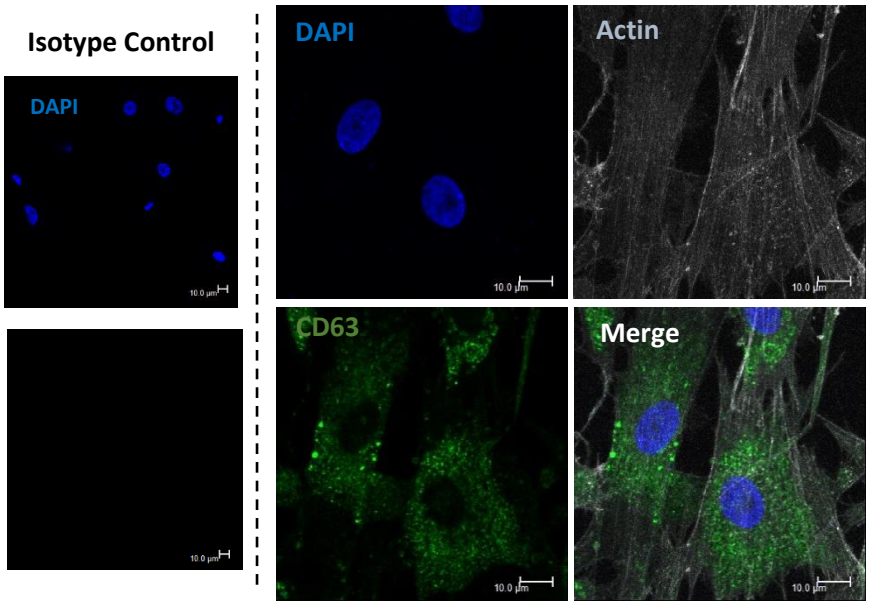

Figure 13 - ICC of CD63 marked HPASMCs before EVs release. DAPI marks nuclei, Actin for cytoskeleton, CD63 for EVs.

4.2 PHK67 labelled HPASMCs-EVs can bind HPAECs' membrane

As initial method to study the HPASMCs-HPAECs communication during PAH conditions, HPASMC-EVs were firstly labelled, as mentioned in the previous section. Then, HPAECs were treated with the labeller EVs (PKH67 free dye was used as control). Yellow-green fluorescent dots, with EVs average size, were found on the HPAECs´ membrane as showed in Figure 14. This result demonstrates that the structure of HPASMC-EVs can bind HPAECs although, false positives cannot be excluded since proteins in the cells´media have been shown to bind the dye [45], the negative control carried out with PKH67 dye alone did not show any evidence of green fluorescence (Figure 14). Next step would be to make this result more robust, using a more reliable method, as well as to demonstrate they are functionally taken up.

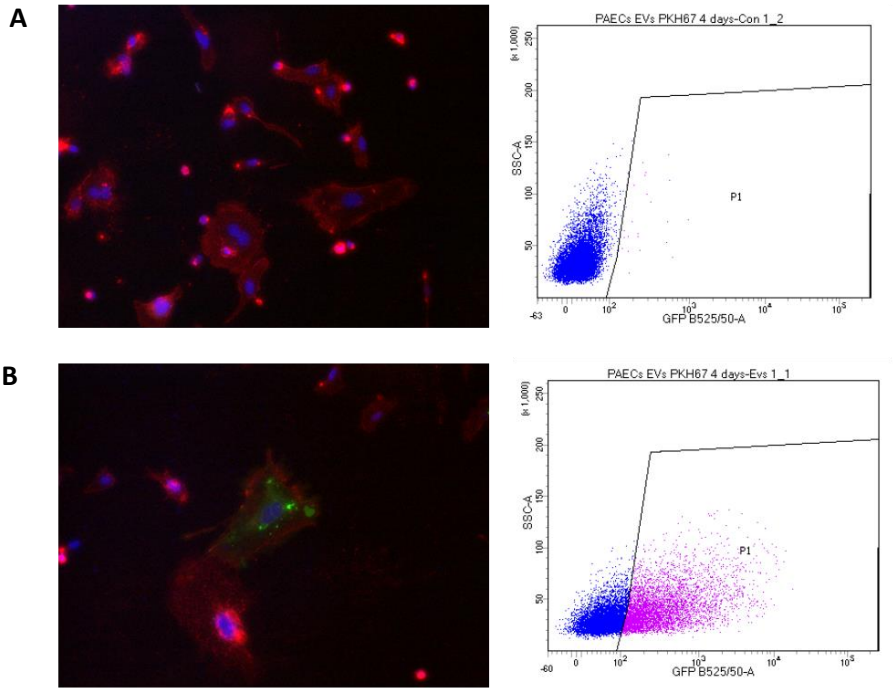

Figure 14 - PKH67 staining of EVs showed by fluorescence microscope and FACS. ***A****. Control;* ***B.*** *GFP⁺ EVs taken up by HPAECs*

4.3 The Cre-Lox*P* method shows HPAECs take up HPASMC-EVs by fluorescence colour switch

This method has been used to confirm what was already seen with PKH67 staining of EVs but in a more reliable and robust fashion. Moreover, this method provides evidence of the translation of mRNA into protein in the recipient cell, which involves functional transport. To demonstrate *in vitro* transport of EVs from HPASMCs to HPAECs during PAH, Dr Fernando De la Cuesta, from the Baker's Laboratory, optimised the above described Cre-Lox*P* method [52] to apply it for the first time in vascular primary cell models [53]. The vector to generate Cre^+ donor cells is a lentivirus (LV-CMV-nlsCre, known to be constitutively expressed thanks

to a CMV immediate early promoter cassette) and with high efficiency in gene delivery to primary vascular cells. HPASMC–Cre^{+}-EVs isolated from the HPASMCs-Cre^{+} supernatant, were checked for the presence of Cre mRNA by qRT-PCR. Results showed that Cre mRNA is efficiently loaded into EVs (Figure 15). Following LV-mediated infection of HPASMCs. HPASMCs-Cre^{+} and HPAECs-Rep^{+} were co-cultured. The appropriate MOI for transducing both HPASMCs and HPAECs was firstly tested in order to avoid spontaneous background recombination events. MOI tested were between 0.1 and 3; therefore, MOI= 0.1 for HPAECs and MOI=0.5 for HPASMCs were chosen since not any background recombination was detected. In these conditions, significant Cre-mediated recombination compared to Control cultures from HPASMCs-Null: HPAECs-Rep^{+} and HPAECs Rep^{+} cells alone was observed (Figure 16). With this improved method, it has been possible to visualise, for the first time, *in vitro* functional communication between HPASMCs and HPAECs (vascular cell types involved in PAH), demonstrating transfer and translation of Cre mRNA through EVs, resulting in protein expression in recipient cells.

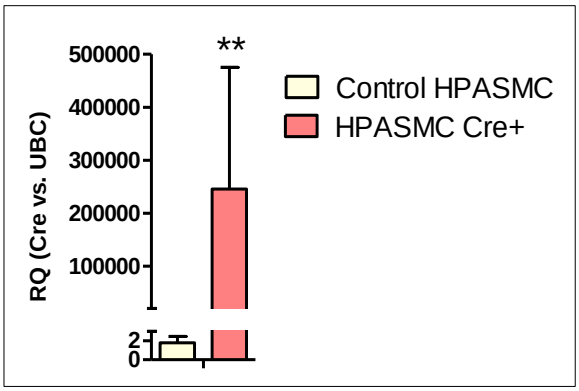

Figure 15 – qRT-PCR of Cre mRNA detected in EVs, with control.

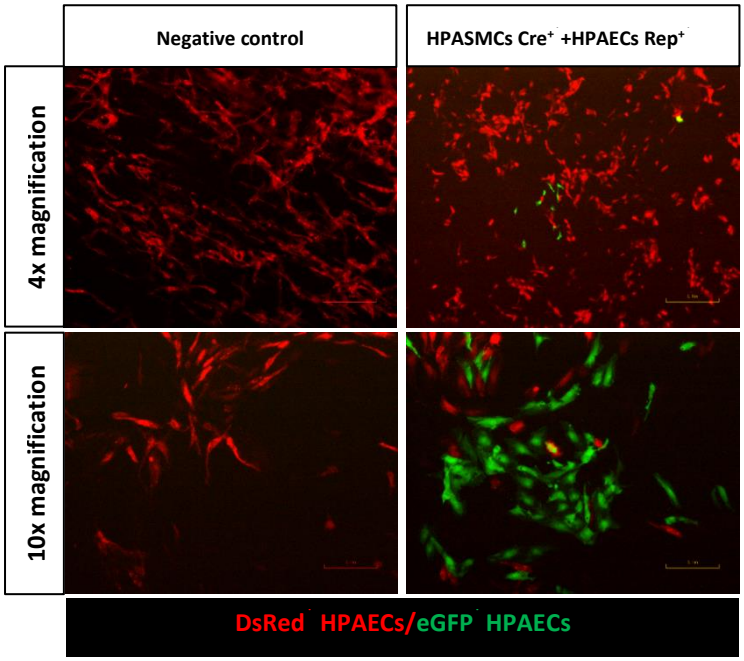

Figure 16 - EV-mediated transfer of Cre mRNA from HPASMCs to HPAECs in normal conditions

As previously said in the *Materials and Methods* chapter, distal cell-cell communication in transwell co-cultures was also investigated.

In this case, this system did not seem to work efficiently, only showing occasionally some green cells, probably due to these specific cell types being close one to another in the vascular bed, where distance is shorter, and communication may occur mainly locally. Pictures obtained by fluorescence microscopy (Figure 17B) indicate the occurrence of some green fluorescent cells, although it was not possible to see a significant increase with FACS analysis (Figure 17A).

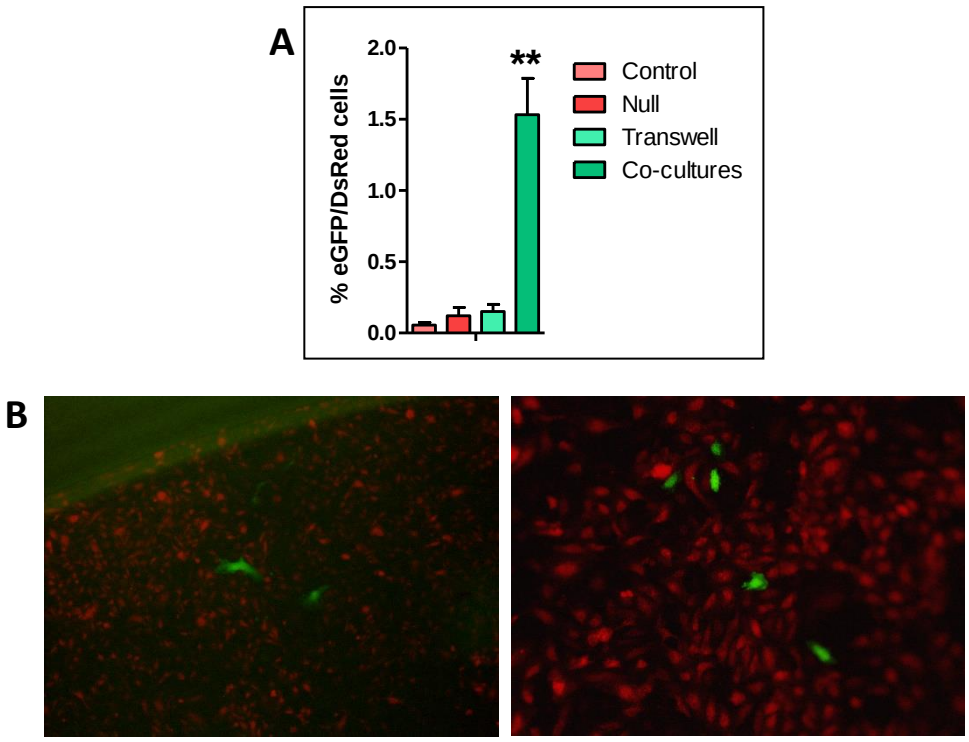

*Figure 17 - **A**, graph image percentage of eGFP⁺ cells measured by FACS in 4 different conditions: Control, Null, Transwell and in co-cultures; **B**, inhere some green HPAEC are illustrated. Their amount was too poor to assume the transwells worked efficiently.*

4.4 Communication between HPASMCs and HPAECs is bidirectional

Cell-cell communication experiments have been also performed in the opposite direction, using HPAECs as donor cells whereas HPASMCs were used as recipient cells. These cells were transduced with LV-Cre and LV-Rep⁺ respectively and seeded in close-contact co-cultures. The desired ratio, in terms of greater yield of green cells and absence of background recombination, was 3:1; which is consistent with higher amount of donor cells resulting in increased delivery of EVs to recipient cells. This component was assessed by microscopy and by FACS analysis. Figure 18 shows a representative experiment of bidirectional communication of HPASMCs and HPAECs co-cultures.

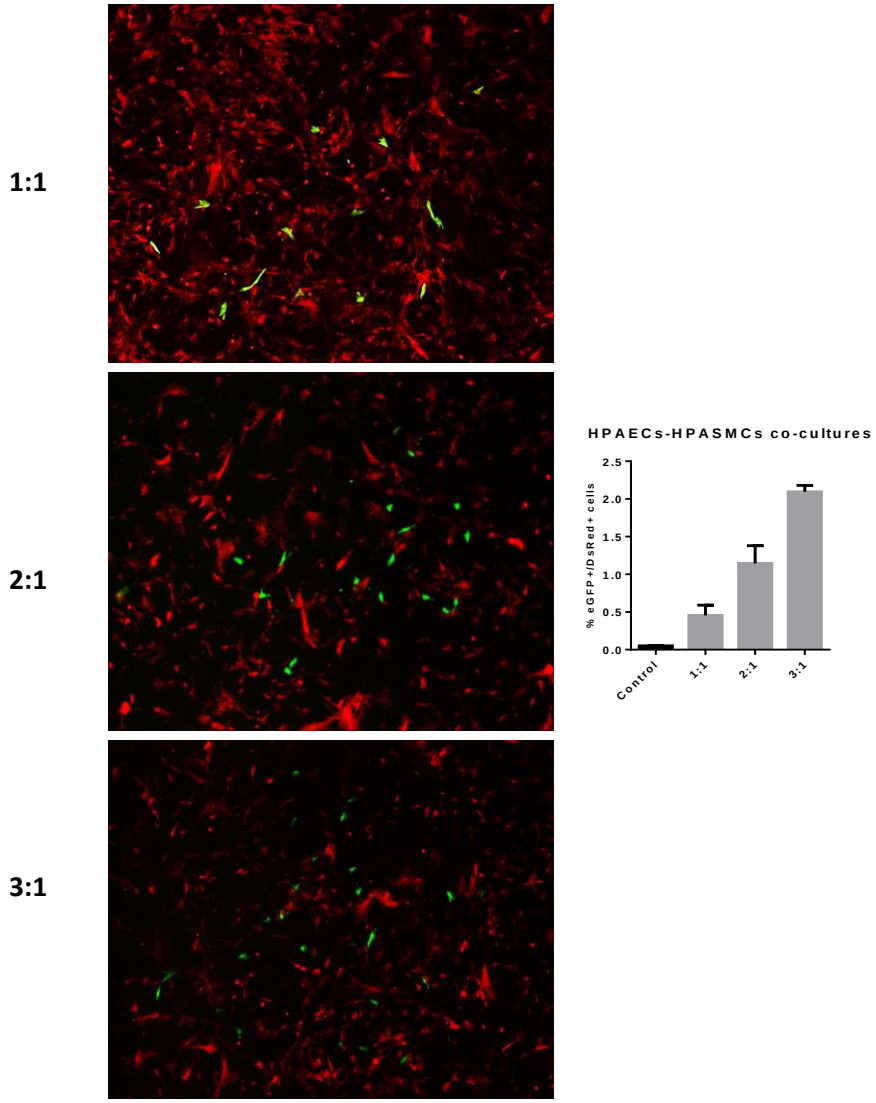

Figure 18 - EVs transport is bi-directional and it is proportional to the number of donor cells seeded. Both HPASMCs to HPAECs and HPAECs to HPASMCs ways gave same results. Graph shows data from a representative experiment. Red cells are Reporter cells and green cells are recipient cells that took up EVs-Cre.

4.5 EV-mediated transfer of mRNA from HPASMCs to HPAECs is enhanced by TGFβ1 *in vitro*

Surprisingly, after treating HPASMCs with TGFβ1 and co-culturing them with HPAECs, a substantial increase in the uptake of HPASMC-Cre-EVs was observed. Indeed, results in Figure 19 show significant variation in EVs-RNA with TGFβ1 transfer, but no significant alteration in NTA measurements of EVs/cells released into the supernatant (Control vs TGFβ1). Hence, TGFβ1 enhances transport of EVs from HPASMCs to HPAECs but does not increase release by donor cells, which implies that the enhanced communication is mainly due to the activated state of HPAECs, typical of endothelial dysfunction, increasing EVs´ uptake.

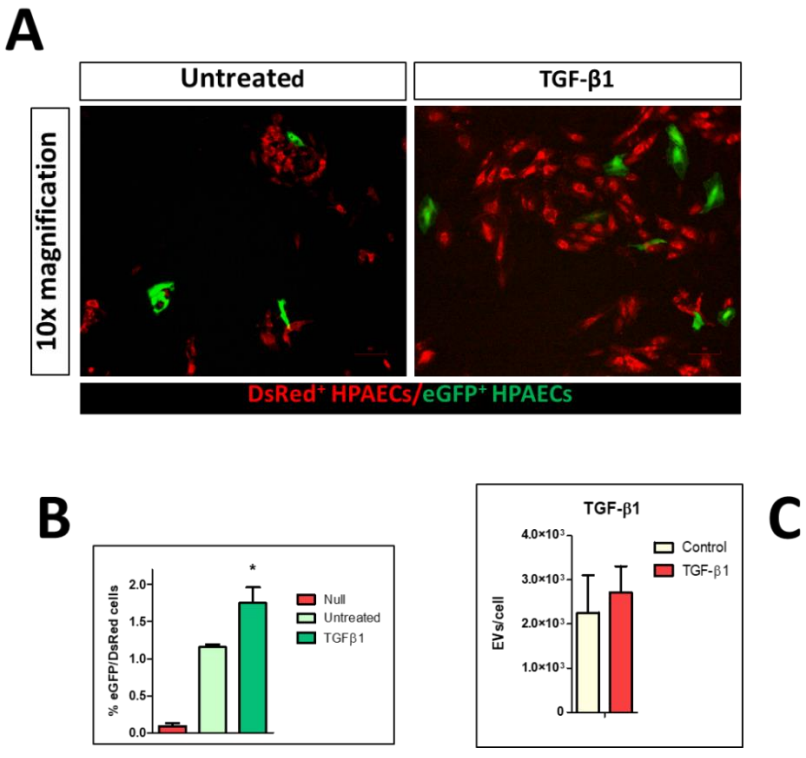

Figure 19 – Uptake of HPASMC-EVs from HPAECs is enhanced by TGFβ1 pre-treatment in vitro. ***A****. Fluorescence microscopy images HPAECs co-cultured with pre-treated HPASMCs;* ***B****, FACS results show a higher % of green cells in TGFβ1 pre-treated co-cultures.* ***C****, NTA shows no alteration of the release of EVs/cell into the supernatant in HPASMCs cultures treated with TGFβ1.*

4.6 HPASMC-TGFβ1-EVs are enriched in TGFβ superfamily ligands GDF11, TGFβ3 and transcription factor Zeb1

In previous work from the Baker's group, Dr Fernando de la Cuesta used low-input RNA-Seq to analyse the RNA cargoes sorted into HPASMC-EVs under basal conditions (Control). RNA-Seq data was analysed by Dr Julie Rodor, detecting a total amount of 2417 genes in HPASMC-EVs and 13867 in cellular RNA. Among these, 759 genes were found significantly enriched in HPASMC-EVs compared to their cells of origin with an EVs-characteristic overrepresentation of pseudogenes (Figure 20). This suggests that EVs are loaded with their own specific transcriptome.

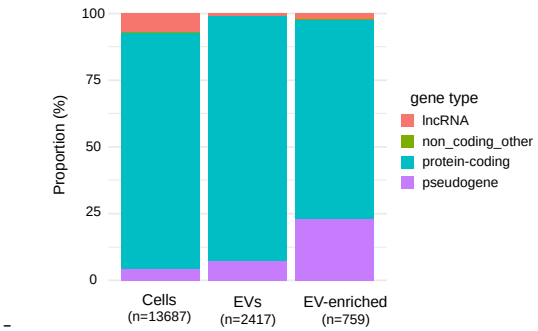

Figure 20 - Characterisation of the genes obtained by RNA-Seq: EVs enrichment column shows what is differential in EVs from Cells' extracts. Differences in reads from cells to EVs are due to the amount of starting material.

Interestingly, TGFβ1 stimulation of donor cells, compared to basal conditions, gave EVs a transcriptional signature typical of cells undergoing fibrosis. Furthermore, 90 genes were found differentially expressed in EVs from cells treated with TGFβ1, compared to Control EVs. These upregulated genes include bHLHE40 and

palladin, both connected to mesenchymal-transition as described in the Endothelial-to-Mesenchymal Transition in PAH paragraph.

4.6.1 Volcano Plot

A volcano plot is a type of scatterplot that shows statistical significance (p-value) versus magnitude of change (fold change). It enables quick visual identification of genes with large fold changes that are also statistically significant. In this case, a Volcano plot was made for highlighting those genes resulting enriched or depleted in the EVs samples compared to their cells of origin. This plot (Figure 21) demonstrates that EVs are precisely loaded with certain RNAs, whereas others are specifically not sent into EVs. Highlighted ones are TGFβ3, GDF11 and Zeb1, candidates for further validations.

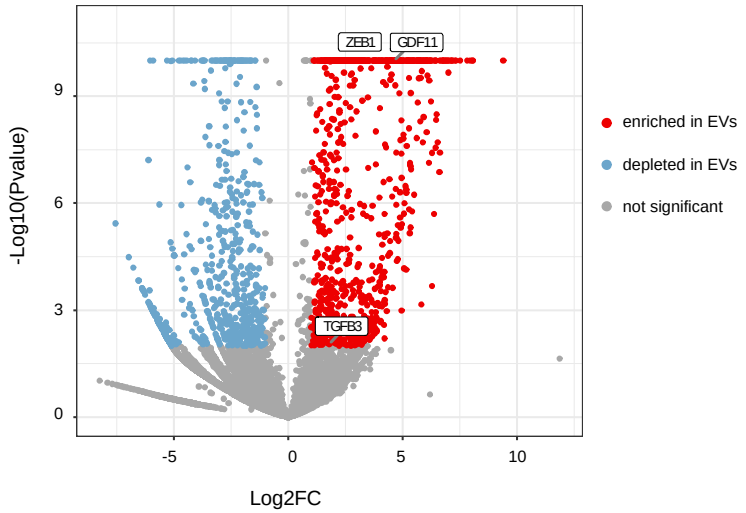

Figure 21 - Volcano plot of EVs' downregulated or overexpressed genes

4.6.2 PCA, Principal Component Analysis

Principal component analysis (PCA) is a statistical procedure that uses an orthogonal transformation to convert a set of observations of possibly correlated variables into a set of values of linearly uncorrelated variables called Principal Compo-

nents (PCs). In a nutshell, PCA captures the essence of the data in a few principal components, which describe the most variation in the dataset. PCA graph in Figure 22 displays 4 conditions (Control cells, TGFβ1 cells and Control and TGFβ1 EVs) clustered by similarities so that the more they are separated/close to each other, the more their cluster is different/analogous. In this case, it is proved that controls and treated cells are distinguished into separated clusters, and also their derived vesicles have peculiar variables and so they appear distant on the graph. At the same time, it is also clear that EVs´ and cells clusters are significantly different one to another, meaning there is a specific RNA composition of EVs compared to their cells of origin, as well as from Control EVs to treated ones.

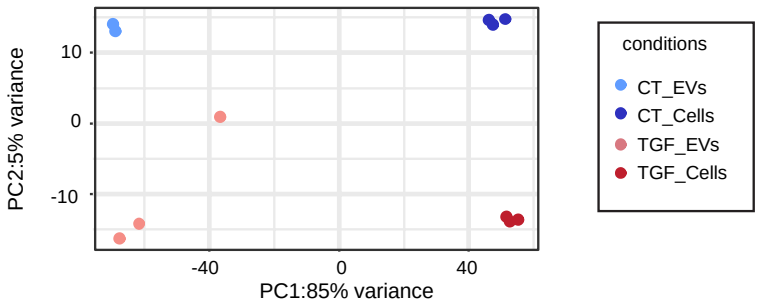

Figure 22 - PCA, Principal Component Analysis describing Control and TGFβ1 treated HPASMCs and derived EVs clusters

4.6.3 Further analysis on enriched cargo in HPASMC-EVs revealed the presence of TGFβ family ligands

Analysing the enriched cargo in normal HPASMC-EVs (so presumably in any EV released by healthy HPASMCs *in vitro*) some interesting RNAs were found: TGFβ3, GDF11 and Zeb1. We further studied these enriched RNAs and their role and expected localisation inside the cell using available databases, finding two of them localised only inside EVs (https://www.proteinatlas.org) (Figure 23). Therefore, this fascinating finding required further attention. qRT-PCR validations were per-

formed, showing high expression levels as predicted by RNA-Seq Analysis. Furthermore, ICC on untreated HPASMCs was performed in order to understand whether the cargoes were also present at the protein level. (Figure 24, Figure 25, Figure 26). Despite the fact that Zeb1 was found co-localised with CD63 within the HPASMCs cytoplasm (that means, before EVs to be released), neither TGFβ3 nor GDF11 were found co-localised inside HPASMCs-EVs analysed.

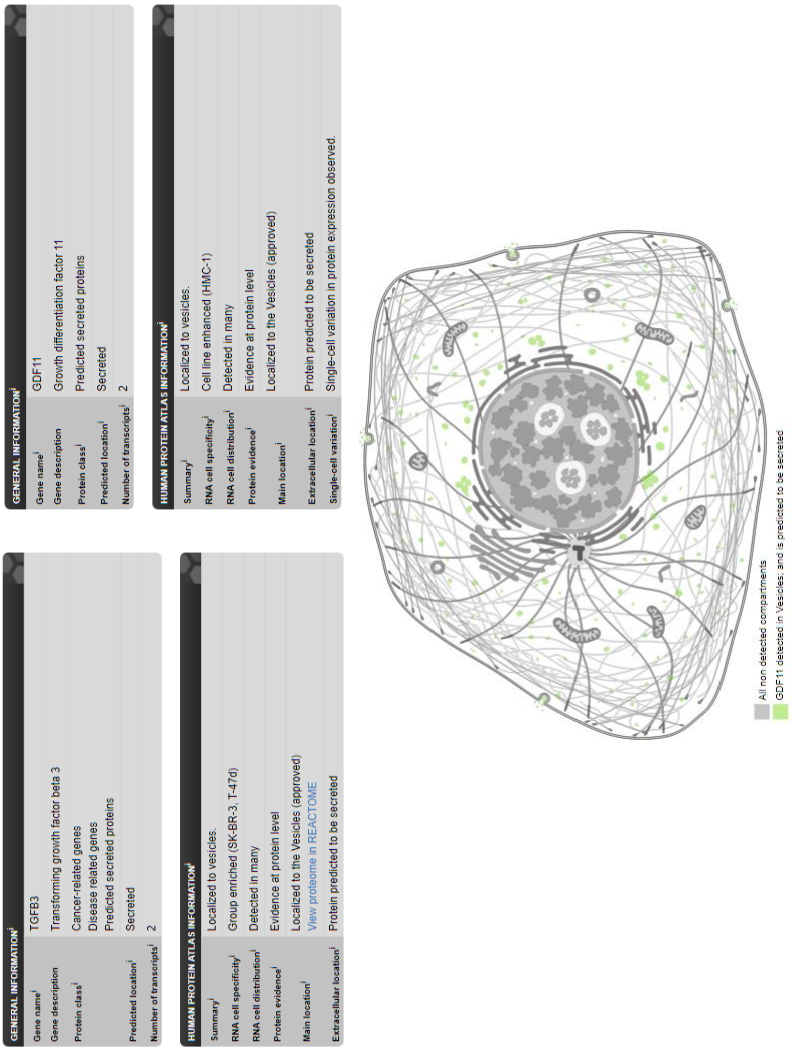

Figure 23 - The Human Protein Atlas finding for GDF11 and TGF-3 in cells localisation

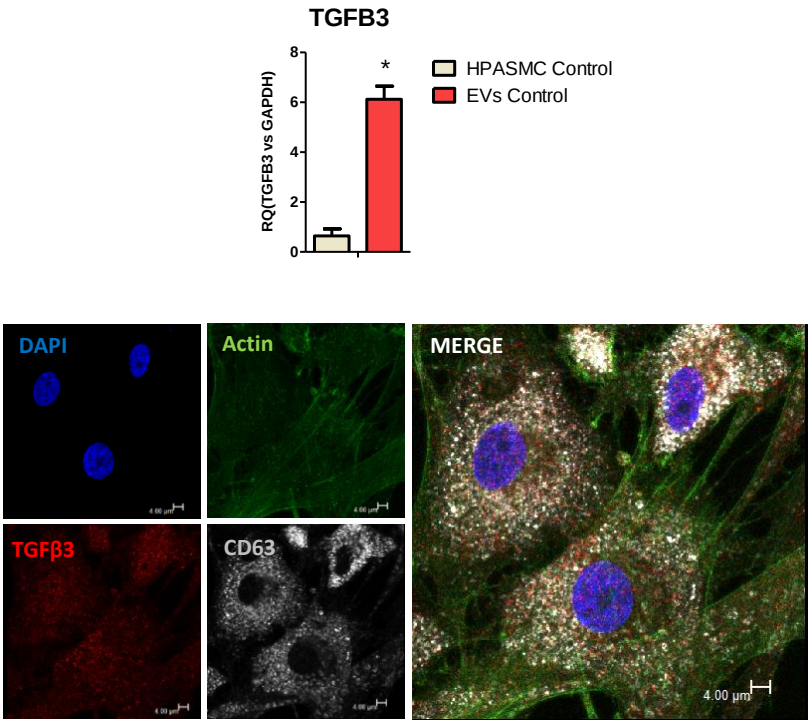

Figure 24 - TGFβ3 Validation and ICC

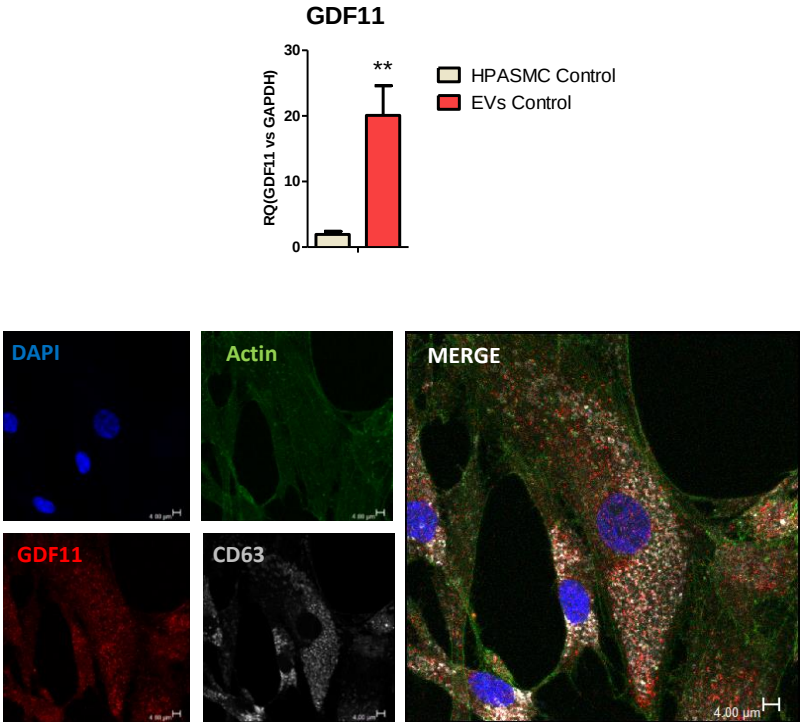

Figure 25 - GDF11 Validation and ICC

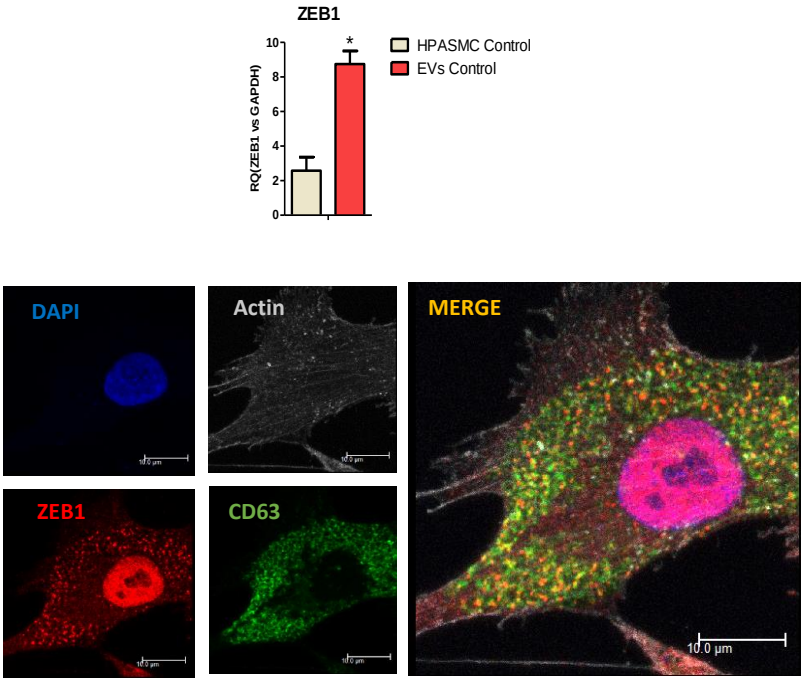

Figure 26 - Zeb1 Validation and ICC

4.7 TGFβ1 treatments lead to the upregulation of bHLHE40 and palladin in HPASMC-EVs

To study the effect of TGFβ1 treatment on the RNA content carried by HPASMC-EVs, the transcriptome of HPASMC-EVs was compared in the two different conditions. 90 differential RNAs were found in TGFβ1-EVs compared to the Control. Biological process Gene Ontology Enrichment analysis (GO Analysis) highlighted differential RNAs found in TGFβ1 EVs to be related to cell differentiation, migration and response to wounding (Figure 27), all distinctive features of cells during PAH. Interaction Network analysis showed a cluster of RNAs related to actin and ECM remodelling (Figure 28– red circle) which is a well-known feature of cells undergoing EndMT and since palladin and bHLHE40 have been found over-represented, they were further investigated because of their documented association with *Epi-*

thelial-to-mesenchymal transition (EMT) [40][41], which may mean they could be involved also in EndMT. (Palladin is highlighted with a black circle). Therefore, RNA validations were made by means of qRT-PCR, in order to exclude technical artefacts and validate the results in a greater cohort of samples. The bar chart shows palladin and bHLHLE40 are overexpressed in both TGFβ1 donor cells and derived EVs (Figure 29A and B, respectively).

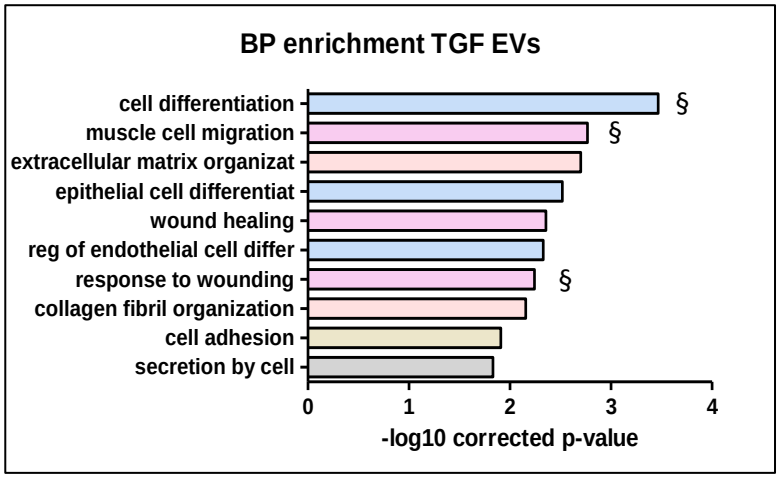

Figure 27 - GO Analysis shows pathways activated or in which TGFβ1 cargo is involved

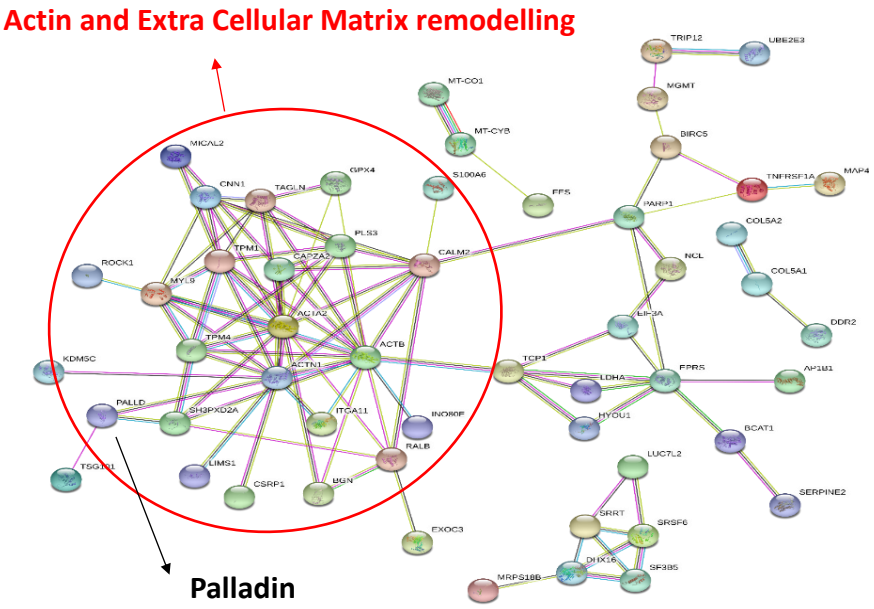

Figure 28 - Interaction Network

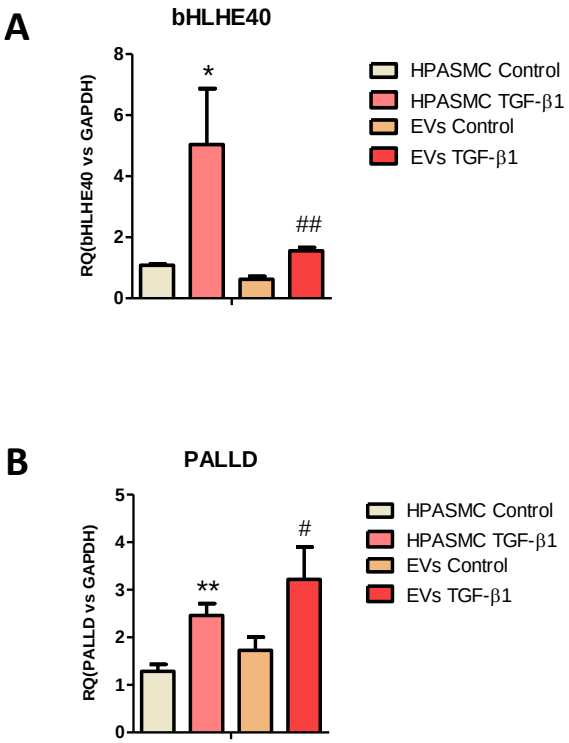

Figure 29 - qRT-PCR of bHLHE40 (A) and palladin (B)

These results together point out that TGFβ1-EVs carry overexpressed RNAs involved in molecular pathways connected to induction of pro-fibrotic effects that could drive healthy HPAECs to exacerbate or initiate PAH involved pathways.

For these reasons, the following preliminary investigations were conducted.

4.8 Visual Phenotypic Changes in HPAECs treated with HPASMCs-EVs

These preliminary studies were performed to investigate the hypothesis whether HPASMC-TGFβ1-EVs could be capable of driving recipient cells to start or exacerbate a PAH or EndMT phenotype. Pictures here below illustrate an early phenotypic transition visually observed under the optical microscope. HPASMC-TGFβ1-EVs treated HPAECs are more elongated and show a more mesenchymal spindle-like morphology compared to the Control HPAECs. Nevertheless, these were preliminary experiments that need to be confirmed and further investigated using functional assays.

Furthermore, the chance of the exacerbation hypothesis was also investigated in parallel, with an EndMT *in vitro* model. Preliminary results also suggested that HPASMC-TGFβ1-EVs could accelerate the EndMT process already taking place (Figure 30).

These samples were also investigated by means of qRT-PCR to examine any possible misregulated EndMT marker. qRT-PCRs showed a surprisingly significative up-regulation of collagen A (COL1A) and actin 2 (ACTA2) while they do not change in Control HPAECs, indicating a probable incrementation in the transition to the mesenchymal phenotype significance due to the HPASMC-TGFβ1-EVs uptake (results not shown). As already discussed in Paragraph 4.7 in Results section, HPASMC-TGFβ1-EVs are loaded with mRNAs known to be involved in EMT, prob-

ably also in EndMT, that may lead HPAECs to a mesenchymal phenotype and morphology. Although these findings might be interesting, this experiment was difficult to reproduce because of different factors, such as: 1. When using an EndMT model, it is difficult to control its efficiency and set up an ”early stage” in order to see appreciable differences produced by EVs. 2. EndMT enhancing factors may variate from batch-to-batch of HPASMC-EVs and their effects on HPAECs may not be always evident.

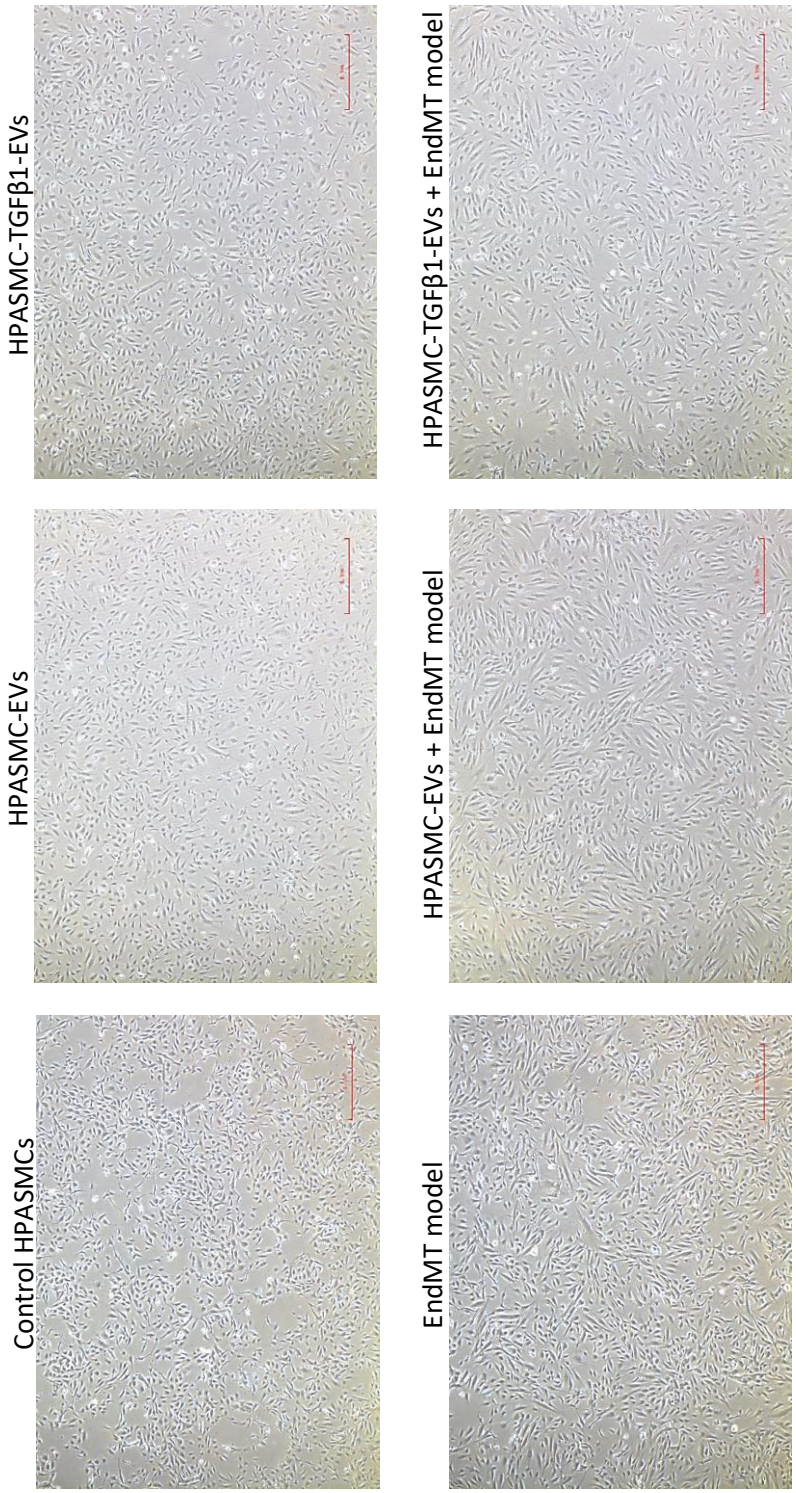

Figure 30 - HPAECs treated with HPASMC-EVs; EVs seem to induce phenotypic changes in HPAECs. HPAECs cultured alone, with HPASMC-EVs or HPASMC-TGFß1-EVs. Also, simulating EndMT in vitro by cytokines treatments, both HPASMC-EVs and HPASMC-TGFß1-EVs increase the EndMT state. Change in phenotype by eye seems evident, but further investigations are needed

5 Discussion

The main objective of this project was to investigate the involvement of EVs-mediated communication during Pulmonary Arterial Hypertension through cutting-edge technologies, such as the Cre-Lox*P* method to image the EVs´ uptake and transcriptomic analysis of EVs' cargo.

Two different conditions were investigated: untreated cells (mimicking physiological conditions) and cells treated by TGFβ1 (as an excessive TGFβ1 production is associated with fibrotic diseases and also with PAH [56]). Firstly, HPASMCs treated or not treated with TGFβ1 were characterised through Nanosight measurements to obtain EVs´ concentration and EVs´ dimension profile, and western blot and ICC to confirm CD63 presence at protein level as EVs marker. First try of imaging EVs´ uptake has been made by using PKH67 staining. Additionally, using the Cre-Lox*P* method, optimised previously in the lab for the application on primary cells, it was possible for the first time to track the uptake of EVs. The presence of mRNA-Cre cargo on HPASMC-EVs was confirmed by qRT-PCR, and its functionality was demonstrated in co-cultured cells by the switch of recipient cells' colour from red to green, indicating the enzyme was actively capable to cut the floxed sites on the Reporter cells' construct. Another finding was that HPASMCs-HPAECs communication EVs-mediated is bi-directional and it follows a dose-dependent trend. It was also observed, that EV-mediated transfer of mRNA from HPASMCs to HPAECs is enhanced by *in vitro* administration of TGFβ1. This, together with the fact that treated HPASMCs don´t increase release of EVs, proves that activated HPAECs gain the capability to take up more EVs than cells in normal conditions.

Therefore, during PAH, altered/inflammatory state surrounding endothelial cells is likely to modulate their response to HPASMC-EVs´cargo.

Next, the RNA diversity between healthy EVs and EVs during TGFβ1-signalling altered conditions was investigated. The two EVs´ types showed different transcriptome, which was also different from that of their HPASMCs of origin. Among the enriched cargoes in healthy HPASMC-EVs, some interesting members of TGFβ superfamily were found: TGFβ3, GDF11; as well as Zeb1.

It is well-known that TGFβ3 is highly upregulated in both medial and intimal layers of remodelled pulmonary vessels [56], and important contributor in vascular remodelling during PAH [57] and it was found enriched in EVs from other other cell types (MSCs) [58]. GDF11 has been reported to promote proliferation and abnormal angiogenesis on HPAECs [59], while Zeb1 is a transcription factor known for its master regulator role in EMT and EndMT [22]. Validations of the cargoes by qRT-PCR were then conducted obtaining a significative overexpression of the three of them in HPASMC derived EVs, compared to their donor cells. At this point, next phase was analysing their potential expression at the protein level by means of ICC, that surprisingly revealed no co-localisation with CD63, for all but Zeb1. Therefore, it suggests that only GDF11 and TGFβ3 mRNA is loaded into EVs, but not their proteins.

In *in vitro* PAH conditions, the cargo was analysed by RNA-Seq. To validate interesting RNAs, qRT-PCRs were carried out confirming the overexpression of bHLHE40 and palladin in HPASMC-TGFβ1-EVs. HPAECs´cell cultures treated with HPASMC-TGFβ1-EVs and Control-EVs showed visual phenotypic changes, switching from an endo-to a spindle-shaped cell; potentially indicating a fibrotic effect of those EVs as in EMT/EndMT. Therefore, it is here postulated that this phenotypic change might be due to HPASMC-TGFβ1-EVs RNAs cargo (bHLHE40 and pal-

ladin) effects being them both acknowledged to participate in the transitions from an epithelial to mesenchymal phenotype during EMT and also to the greater uptake of GDF11, TGFβ3 and Zeb1, specifically sorted into both HPASMC- and HPASMC-TGFβ1-EVs.

6 Conclusions

In this thesis, the role of EVs-mediated communication during Pulmunary Arterial Hypertension has been made clearer by demonstrating that:

1. HPASMC-EVs can bind HPAECs membrane as showed by PKH67 labelling;
2. HPASMC-EVs cargo is functional and can be actively translated into protein by recipient cells as demonstrated using the optimised Cre-Lox*P* method on primary cells for the first time;
3. Cell-to-cell transfer and translation of Cre-mRNA from HPASMC-to-HPAECs is enhanced by TGFβ1, thus this enhanced communication may play an important role in PAH, where TGFβ signalling is impaired;
4. The EVs transfer is bi-directional as HPASMCs-to-HPAECs and HPAECs-to-HPASMCs communication experiments pointed out;
5. HPASMC-EVs carry a specific transcriptome which is differential of that of their cells of origin;
6. HPASMC-EVs overexpress members of TGFβ1 superfamily, TGFβ3 and GDF11, and Zeb1 known as master regulator of EndMT, as revelaed by transcriptomic analysis;
7. TGFβ3 and GDF11 are only present at mRNA level, while Zeb1 is surprisingly espressed also at the protein level, as shown by mRNA validation and ICC, and all are selectively loaded into vesicles;
8. HPASMC-TGFβ1-EVs are enriched in RNAs, such as bHLHE40 and palladin, together with the already present TGF-β3, GDF11 and Zeb1, that might contribute to induce or exacerbate EndMT occurring in HPAECs during PAH.

Conclusions

In summary, we have proven that HPAECs can take up HPASMC-EVs and efficiently translate their mRNA cargo through an optimised primary cell Cre-Lox*P* system able to track cells taking up EVs. This uptake is bi-directional and is increased under TGFβ1 treatment. Transcriptomics analysis on Control-EVs revealed that EVs derived from healthy HPASMCs are loaded with TGFβ superfamily ligand RNAs selectively sorted into EVs, although all not present at the protein level, but Zeb1. TGFβ1 treated HPASMCs derived EVs are enriched in RNAs that might contribute to induce or exacerbate EndMT on HPAECs as their fibrotic phenotypic change observed *in vitro* seems to point out.

To conclude, results obtained provide evidence of the biological relevance of EVs-mediated communication within HPASMCs and HPAECs during PAH development and also encourage to continue investigating their interesting role in physiological and pathological conditions performing further functional experiments.

7 Bibliography

[1] R. M. Tuder, 'Pulmonary vascular remodeling in pulmonary hypertension', *Cell and Tissue Research*, vol. 367, no. 3. Springer Verlag, pp. 643–649, 01-Mar-2017.

[2] R. D. Machado *et al.*, 'Genetics and genomics of pulmonary arterial hypertension.', *J. Am. Coll. Cardiol.*, vol. 54, no. 1 Suppl, pp. S32-42, Jun. 2009.

[3] M. J. Kim *et al.*, 'Clinical significance linked to functional defects in bone morphogenetic protein type 2 receptor, BMPR2', *BMB Reports*, vol. 50, no. 6. The Biochemical Society of the Republic of Korea, pp. 308–317, 2017.

[4] E. D. Austin and J. E. Loyd, 'The genetics of pulmonary arterial hypertension', *Circ. Res.*, vol. 115, no. 1, pp. 189–200, Jun. 2014.

[5] D. H. Best, E. D. Austin, W. K. Chung, and C. G. Elliott, 'Genetics of pulmonary hypertension.', *Curr. Opin. Cardiol.*, vol. 29, no. 6, pp. 520–7, Nov. 2014.

[6] R. D. Machado *et al.*, 'Mutations of the TGF-β type II receptor BMPR2 in pulmonary arterial hypertension', *Human Mutation*, vol. 27, no. 2. 2006.

[7] J. E. Loyd, M. G. Butler, T. M. Foroud, P. M. Conneally, J. A. Phillips, and J. H. Newman, 'Genetic anticipation and abnormal gender ratio at birth in familial primary pulmonary hypertension.', *Am. J. Respir. Crit. Care Med.*, vol. 152, no. 1, pp. 93–7, Jul. 1995.

[8] R. D. Machado *et al.*, 'Genetics and Genomics of Pulmonary Arterial Hypertension', *J. Am. Coll. Cardiol.*, vol. 54, no. 1, pp. S32–S42, Jun. 2009.

[9] A. Weiss and L. Attisano, 'The TGFbeta superfamily signaling pathway',

Wiley Interdisciplinary Reviews: Developmental Biology, vol. 2, no. 1. pp. 47–63, Jan-2013.

[10] N. Rol, K. B. Kurakula, C. Happé, H. J. Bogaard, and M. J. Goumans, 'TGF-β and BMPR2 signaling in PAH: Two black sheep in one family', *International Journal of Molecular Sciences*, vol. 19, no. 9. MDPI AG, 01-Sep-2018.

[11] J. Massagué, 'TGF-β signaling in development and disease', *FEBS Lett.*, vol. 586, no. 14, pp. 1833–1833, Jul. 2012.

[12] J. Massagué, 'Integration of Smad and MAPK pathways: A link and a linker revisited', *Genes and Development*, vol. 17, no. 24. pp. 2993–2997, 15-Dec-2003.

[13] G. J. Prud'homme, 'Pathobiology of transforming growth factor beta in cancer, fibrosis and immunologic disease, and therapeutic considerations.', *Lab. Invest.*, vol. 87, no. 11, pp. 1077–91, Nov. 2007.

[14] N. W. Morrell *et al.*, 'Cellular and Molecular Basis of Pulmonary Arterial Hypertension', *Journal of the American College of Cardiology*, vol. 54, no. 1 SUPPL. 1. 30-Jun-2009.

[15] N. W. Morrell *et al.*, 'Altered growth responses of pulmonary artery smooth muscle cells from patients with primary pulmonary hypertension to transforming growth factor-β1 and bone morphogenetic proteins', *Circulation*, vol. 104, no. 7, pp. 790–795, Aug. 2001.

[16] Y. Y. Zhao and A. B. Malik, 'A Novel Insight Into the Mechanism of Pulmonary Hypertension Involving Caveolin-1 Deficiency and Endothelial Nitric Oxide Synthase Activation', *Trends in Cardiovascular Medicine*, vol. 19, no. 7. pp. 238–242, Oct-2009.

[17] S. Eddahibi *et al.*, 'Cross talk between endothelial and smooth muscle cells in pulmonary hypertension: Critical role for serotonin-induced smooth

muscle hyperplasia', *Circulation*, vol. 113, no. 15, pp. 1857–1864, Apr. 2006.

[18] J. Folkman and P. A. D'Amore, 'Blood vessel formation: what is its molecular basis?', *Cell*, vol. 87, no. 7, pp. 1153–5, Dec. 1996.

[19] K. Teichert-Kuliszewska *et al.*, 'Bone morphogenetic protein receptor-2 signaling promotes pulmonary arterial endothelial cell survival: Implications for loss-of-function mutations in the pathogenesis of pulmonary hypertension', *Circ. Res.*, vol. 98, no. 2, pp. 209–217, Feb. 2006.

[20] G. L. Wang, B. H. Jiang, E. A. Rue, and G. L. Semenza, 'Hypoxia-inducible factor 1 is a basic-helix-loop-helix-PAS heterodimer regulated by cellular O 2 tension', *Proc. Natl. Acad. Sci. U. S. A.*, vol. 92, no. 12, pp. 5510–5514, Jun. 1995.

[21] G. L. Semenza, 'Hypoxia-inducible factors in physiology and medicine', *Cell*, vol. 148, no. 3. pp. 399–408, 03-Feb-2012.

[22] J. C. Kovacic *et al.*, 'Endothelial to Mesenchymal Transition in Cardiovascular Disease: JACC State-of-the-Art Review.', *J. Am. Coll. Cardiol.*, vol. 73, no. 2, pp. 190–209, Jan. 2019.

[23] J. G. Cho, A. Lee, W. Chang, M. S. Lee, and J. Kim, 'Endothelial to mesenchymal transition represents a key link in the interaction between inflammation and endothelial dysfunction', *Frontiers in Immunology*, vol. 9, no. FEB. Frontiers Media S.A., 20-Feb-2018.

[24] J. C. Kovacic, N. Mercader, M. Torres, M. Boehm, and V. Fuster, 'Epithelial-to-mesenchymal and endothelial-to-mesenchymal transition from cardiovascular development to disease', *Circulation*, vol. 125, no. 14, pp. 1795–1808, Apr. 2012.

[25] M. Yáñez-Mó *et al.*, 'Biological properties of extracellular vesicles and their

physiological functions', *Journal of Extracellular Vesicles*, vol. 4, no. 2015. Co-Action Publishing, pp. 1–60, 2015.

[26] D. Nieri, T. Neri, S. Petrini, B. Vagaggini, P. Paggiaro, and A. Celi, 'Cell-derived microparticles and the lung', *European Respiratory Review*, vol. 25, no. 141. European Respiratory Society, pp. 266–277, 01-Sep-2016.

[27] M. Colombo, G. Raposo, and C. Théry, 'Biogenesis, Secretion, and Intercellular Interactions of Exosomes and Other Extracellular Vesicles', *Annu. Rev. Cell Dev. Biol.*, vol. 30, no. 1, pp. 255–289, Oct. 2014.

[28] B. Pezzuto *et al.*, 'Circulating biomarkers in pulmonary arterial hypertension: update and future direction.', *J. Heart Lung Transplant.*, vol. 34, no. 3, pp. 282–305, Mar. 2015.

[29] A. Giaid *et al.*, 'Expression of endothelin-1 in the lungs of patients with pulmonary hypertension.', *N. Engl. J. Med.*, vol. 328, no. 24, pp. 1732–9, Jun. 1993.

[30] A. L. Cooper and D. Beasley, 'Hypoxia stimulates proliferation and interleukin-1alpha production in human vascular smooth muscle cells.', *Am. J. Physiol.*, vol. 277, no. 4, pp. H1326-37, 1999.

[31] M. Humbert *et al.*, 'Increased interleukin-1 and interleukin-6 serum concentrations in severe primary pulmonary hypertension.', *Am. J. Respir. Crit. Care Med.*, vol. 151, no. 5, pp. 1628–31, May 1995.

[32] P. Libby, S. J. Warner, and G. B. Friedman, 'Interleukin 1: a mitogen for human vascular smooth muscle cells that induces the release of growth-inhibitory prostanoids.', *J. Clin. Invest.*, vol. 81, no. 2, pp. 487–98, Feb. 1988.

[33] M. Rabinovitch, S. G. Haworth, A. R. Castaneda, A. S. Nadas, and L. M. Reid, 'Lung biopsy in congenital heart disease: a morphometric approach

to pulmonary vascular disease.', *Circulation*, vol. 58, no. 6, pp. 1107–22, Dec. 1978.

[34] T. K. Jeffery and J. C. Wanstall, 'Pulmonary vascular remodeling: a target for therapeutic intervention in pulmonary hypertension.', *Pharmacol. Ther.*, vol. 92, no. 1, pp. 1–20, Oct. 2001.

[35] A. S. Leroyer *et al.*, 'Cellular origins and thrombogenic activity of microparticles isolated from human atherosclerotic plaques.', *J. Am. Coll. Cardiol.*, vol. 49, no. 7, pp. 772–7, Feb. 2007.

[36] S. F. Mause *et al.*, 'Platelet microparticles enhance the vasoregenerative potential of angiogenic early outgrowth cells after vascular injury.', *Circulation*, vol. 122, no. 5, pp. 495–506, Aug. 2010.

[37] M. Pérez-Casal, C. Downey, B. Cutillas-Moreno, M. Zuzel, K. Fukudome, and C. H. Ton, 'Microparticle-associated endothelial protein C receptor and the induction of cytoprotective and anti-inflammatory effects', *Haematologica*, vol. 94, no. 3, pp. 387–394, Mar. 2009.

[38] F. Vacante, L. Denby, J. C. Sluimer, and A. H. Baker, 'The function of miR-143, miR-145 and the MiR-143 host gene in cardiovascular development and disease.', *Vascul. Pharmacol.*, vol. 112, pp. 24–30, 2019.

[39] L. Deng *et al.*, 'MicroRNA-143 Activation Regulates Smooth Muscle and Endothelial Cell Crosstalk in Pulmonary Arterial Hypertension', *Circ. Res.*, vol. 117, no. 10, pp. 870–883, 2015.

[40] J. M. Aliotta *et al.*, 'Exosomes induce and reverse monocrotaline-induced pulmonary hypertension in mice', *Cardiovasc. Res.*, vol. 110, no. 3, pp. 319–330, Jun. 2016.

[41] L. Deng *et al.*, 'MicroRNA-143 Activation Regulates Smooth Muscle and Endothelial Cell Crosstalk in Pulmonary Arterial Hypertension', *Circ. Res.*,

vol. 117, no. 10, pp. 870–883, Oct. 2015.

[42] Y. Bei, P. Yu, D. Cretoiu, S. M. Cretoiu, and J. Xiao, 'Exosomes-based biomarkers for the prognosis of cardiovascular diseases', in *Advances in Experimental Medicine and Biology*, vol. 998, Springer New York LLC, 2017, pp. 71–88.

[43] J. Chen *et al.*, 'Therapeutic effects of mesenchymal stem cell-derived microvesicles on pulmonary arterial hypertension in rats.', *Acta Pharmacol. Sin.*, vol. 35, no. 9, pp. 1121–8, Sep. 2014.

[44] J. L. Hewes and N. N. Bauer, 'Extracellular vesicles in pulmonary hypertension: lessons from mesenchymal stromal cell-derived exosomes.', *Am. J. Physiol. Lung Cell. Mol. Physiol.*, vol. 316, no. 5, pp. L720–L722, May 2019.

[45] K. Takov, D. M. Yellon, and S. M. Davidson, 'Confounding factors in vesicle uptake studies using fluorescent lipophilic membrane dyes', *J. Extracell. Vesicles*, vol. 6, no. 1, pp. 1–15, 2017.

[46] A. Zomer *et al.*, 'In vivo imaging reveals extracellular vesicle-mediated phenocopying of metastatic behavior', *Cell*, vol. 161, no. 5, pp. 1046–1057, May 2015.

[47] K. Ridder *et al.*, 'Extracellular vesicle-mediated transfer of functional RNA in the tumor microenvironment mediated transfer of functional RNA in the tumor microenvironment Extracellular vesicle-mediated transfer of functional RNA in the tumor microenvironment', 2015.

[48] J. Lötvall *et al.*, 'Minimal experimental requirements for definition of extracellular vesicles and their functions: A position statement from the International Society for Extracellular Vesicles', *Journal of Extracellular Vesicles*, vol. 3, no. 1. Co-Action Publishing, 2014.

[49] J. K. Actor, 'Immunoassays', in *Elsevier's Integrated Review Immunology and Microbiology*, Elsevier, 2012, pp. 71–79.

[50] J. O. Richards, J. Treisman, N. Garlie, J. P. Hanson, and M. K. Oaks, 'Flow cytometry assessment of residual melanoma cells in tumor-infiltrating lymphocyte cultures', *Cytom. Part A*, vol. 81 A, no. 5, pp. 374–381, May 2012.

[51] A. H. Schönthal, P. Pozarowski, and Z. Darzynkiewicz, 'Analysis of Cell Cycle by Flow Cytometry 301 301 Analysis of Cell Cycle by Flow Cytometry', *Checkp. Control. Cancer*, vol. 281, pp. 301–312, 2004.

[52] A. Zomer, S. C. Steenbeek, C. Maynard, and J. Van Rheenen, 'Studying extracellular vesicle transfer by a Cre-loxP method', *Nat. Protoc.*, vol. 11, no. 1, pp. 87–101, Jan. 2016.

[53] L. B. De la Cuesta, Fernando; Passalacqua, Ilaria; Rodor, Julie; Bhushan, Raghu; Denby and A. H., 'Extracellular vesicle cross-talk from pulmonary artery smooth muscle cells to endothelium in vascular remodelling: effects of excessive TGF-β signaling', *Cell Commun. Signal.*, p. Accepted, In press, 2019.

[54] Y. Wu *et al.*, 'Podoplanin-mediated TGF-β-induced epithelial-mesenchymal transition and its correlation with bHLH transcription factor DEC in TE-11 cells', *Int. J. Oncol.*, vol. 48, no. 6, pp. 2310–2320, 2016.

[55] Y. Wu *et al.*, 'The BHLH transcription factor DEC1 plays an important role in the epithelial-mesenchymal transition of pancreatic cancer.', *Int. J. Oncol.*, vol. 41, no. 4, pp. 1337–46, Oct. 2012.

[56] P. D. Upton and N. W. Morrell, 'The transforming growth factor-β-bone morphogenetic protein type signalling pathway in pulmonary vascular homeostasis and disease', *Exp. Physiol.*, vol. 98, no. 8, pp. 1262–1266, Aug.

2013.

[57] L.-M. Yung, I. Nikolic, S. D. Paskin-Flerlage, R. S. Pearsall, R. Kumar, and P. B. Yu, 'A Selective Transforming Growth Factor-β Ligand Trap Attenuates Pulmonary Hypertension.', *Am. J. Respir. Crit. Care Med.*, vol. 194, no. 9, pp. 1140–1151, 2016.

[58] A. Eirin *et al.*, 'MicroRNA and mRNA cargo of extracellular vesicles from porcine adipose tissue-derived mesenchymal stem cells.', *Gene*, vol. 551, no. 1, pp. 55–64, Nov. 2014.

[59] X. Yu *et al.*, 'Growth Differentiation Factor 11 Promotes Abnormal Proliferation and Angiogenesis of Pulmonary Artery Endothelial Cells.', *Hypertens. (Dallas, Tex. 1979)*, vol. 71, no. 4, pp. 729–741, 2018.

Publications and posters

"Extracellular vesicle cross-talk from pulmonary artery smooth muscle cells to endothelium in vascular remodelling: effects of excessive TGF-β signalling".

De la Cuesta F, Passalacqua I, Rodor J, Bhushan R, Denby L, Baker AH

Cell Communication and Signaling, 2019: Accepted, In press

"*A potential role for extracellular vesicle-mediated communication from smooth muscle cells to endothelial cells in human pulmonary arterial hypertension.*"

Ilaria Passalacqua, Julie Rodor, Raghu Bhushan, Fernando de la Cuesta, Andrew H. Baker

ESM-EVBO Conference 2019, (poster presentation)

"A potential role for extracellular vesicles in smooth muscle cells-endothelial cells communication during human pulmonary arterial hypertension"

Ilaria Passalacqua, Julie Rodor, Raghu Bhushan, Fernando de la Cuesta, Andrew H. Baker

1st EVIta Conference 2019, (poster presentation)